Flow Through The Canso Causeway

Gary L. Bugden, Brent A. Law, Edward P.W. Horne and Shawn E. Roach

Science Branch
Maritimes Region
Coastal Ecosystem Science Division
Fisheries and Oceans Canada
Bedford Institute of Oceanography
PO Box 1006
Dartmouth, Nova Scotia,
B2Y 4A2

2020

Canadian Technical Report of
Fisheries and Aquatic Sciences 3393

Fisheries and Oceans Canada | Pêches et Océans Canada

Canada

Canadian Technical Report of Fisheries and Aquatic Sciences

Technical reports contain scientific and technical information that contributes to existing knowledge but which is not normally appropriate for primary literature. Technical reports are directed primarily toward a worldwide audience and have an international distribution. No restriction is placed on subject matter and the series reflects the broad interests and policies of Fisheries and Oceans Canada, namely, fisheries and aquatic sciences.

Technical reports may be cited as full publications. The correct citation appears above the abstract of each report. Each report is abstracted in the data base *Aquatic Sciences and Fisheries Abstracts*.

Technical reports are produced regionally but are numbered nationally. Requests for individual reports will be filled by the issuing establishment listed on the front cover and title page.

Numbers 1-456 in this series were issued as Technical Reports of the Fisheries Research Board of Canada. Numbers 457-714 were issued as Department of the Environment, Fisheries and Marine Service, Research and Development Directorate Technical Reports. Numbers 715-924 were issued as Department of Fisheries and Environment, Fisheries and Marine Service Technical Reports. The current series name was changed with report number 925.

Rapport technique canadien des sciences halieutiques et aquatiques

Les rapports techniques contiennent des renseignements scientifiques et techniques qui constituent une contribution aux connaissances actuelles, mais qui ne sont pas normalement appropriés pour la publication dans un journal scientifique. Les rapports techniques sont destinés essentiellement à un public international et ils sont distribués à cet échelon. II n'y a aucune restriction quant au sujet; de fait, la série reflète la vaste gamme des intérêts et des politiques de Pêches et Océans Canada, c'est-à-dire les sciences halieutiques et aquatiques.

Les rapports techniques peuvent être cités comme des publications à part entière. Le titre exact figure au-dessus du résumé de chaque rapport. Les rapports techniques sont résumés dans la base de données *Résumés des sciences aquatiques et halieutiques.*

Les rapports techniques sont produits à l'échelon régional, mais numérotés à l'échelon national. Les demandes de rapports seront satisfaites par l'établissement auteur dont le nom figure sur la couverture et la page du titre.

Les numéros 1 à 456 de cette série ont été publiés à titre de Rapports techniques de l'Office des recherches sur les pêcheries du Canada. Les numéros 457 à 714 sont parus à titre de Rapports techniques de la Direction générale de la recherche et du développement, Service des pêches et de la mer, ministère de l'Environnement. Les numéros 715 à 924 ont été publiés à titre de Rapports techniques du Service des pêches et de la mer, ministère des Pêches et de l'Environnement. Le nom actuel de la série a été établi lors de la parution du numéro 925.

Canadian Technical Report of
Fisheries and Aquatic Sciences 3393

2020

Flow Through The Canso Causeway

Gary L. Bugden[1], Brent A. Law[1], Edward P.W. Horne[1], Shawn E. Roach[1]

[1] Fisheries and Oceans Canada, Science Branch, Coastal Ecosystem Science Division, 1 Challenger Dr., Dartmouth, Nova Scotia, B2Y 4A2

Cat. No. Fs97-6/3393E-PDF ISBN 978-0-660-35611-2 ISSN 1488-5379

Correct Citation for this publication:

Bugden, G.L., Law, B.A, Horne, E.P.W., Roach, S.E., 2020. Flow Through the Canso Causeway. Can. Tech. Rep. Fish. Aquat. Sci. 3393: vi + 47 p.

TABLE OF CONTENTS

LIST OF FIGURES

LIST OF TABLES

ABSTRACT

Bugden, G.L., Law, B.A, Horne, E.P.W., Roach, S.E., 2020. Flow Through the Canso Causeway. Can. Tech. Rep. Fish. Aquat. Sci. 3393: vi + 47 p.

Although blocked in the 1950's by the Canso Causeway, Canso Strait could potentially be a transport pathway for the spread of Malpeque Disease, an oyster pathogen, from the southern Gulf of Saint Lawrence to the Eastern Shore of Nova Scotia. This report describes a field program conducted from July through November of 2019 to quantify the environmental factors which could conceivably lead to trans-causeway transport.

The report first characterizes the oceanographic conditions on each side of the causeway. Then an attempt is made to quantify possible transport due to each of the following mechanisms: 1) Percolation through the rock fill from which the causeway is constructed. 2) Over-topping of the causeway by wave action during storm events 3) Water passed as part of Canso Canal locking operations.

RÉSUMÉ

Bugden, G.L., Law, B.A, Horne, E.P.W., Roach, S.E., 2020. Flow Through the Canso Causeway. Can. Tech. Rep. Fish. Aquat. Sci. 3393: vi + 47 p.

Même s'il a été bloqué dans les années 1950 par la chaussée de Canso, le détroit de Canso pourrait être une voie de transport permettant la propagation de la maladie de Malpèque, un agent pathogène de l'huître, de la partie sud du golfe du Saint-Laurent jusqu'à la côte est de la Nouvelle-Écosse. Le présent rapport décrit un programme exécuté sur le terrain entre juillet et novembre 2019 pour quantifier les facteurs environnementaux qui pourraient vraisemblablement causer le transport de part et d'autre de la chaussée.

Le rapport décrit d'abord les conditions océanographiques présentes de chaque côté de la chaussée. On tente ensuite de quantifier le transport possible causé par chacun des mécanismes suivants : 1) percolation dans l'enrochement à partir duquel la chaussée est construite; 2) débordement par-dessus la chaussée par l'effet des vagues pendant les tempêtes; et 3) écoulement d'eau dans le cadre des activités d'éclusage du canal de Canso.

1. INTRODUCTION

Recent concerns expressed by DFO's Maritimes Aquaculture Management Division concerning the spread of Malpeque Disease, an oyster pathogen, from the southern Gulf of Saint Lawrence to the Eastern Shore of Nova Scotia revealed that little was known about potential transport through the Strait of Canso. Although blocked in the 1950's by the Canso Causeway, the Strait could possibly be a transport pathway through over-topping of the causeway by wave action during storm events, percolation through the rock fill from which the causeway is constructed and through water passed as part of Canso Canal locking operations.

Canso Strait separates Cape Breton Island from the Nova Scotia peninsula (Figure 1). The Strait is approximately 22 km long, 1.5 km wide and approximately 45 m deep over most of its length. The man-made Canso Causeway crosses the Strait of Canso, carrying the two vehicle traffic lanes of the Trans-Canada Highway as well as the single track mainline of the Cape Breton and Central Nova Scotia Railway. Constructed in an "S" shape, the 1,385 m rock-fill causeway has a crown 40 m wide and a base width of 244 m in waters having a maximum depth of approximately 65 m, making it one of the deepest causeways in the world. Its construction required just over 10 million tons of rock which was quarried from nearby Cape Porcupine.

Earlier engineering studies suggested that ice in the Strait would quickly damage any bridge and causeway construction was officially started at a ceremony on September 16, 1952. The Strait was permanently blocked on Friday, December 10, 1954. Construction was completed on April 13, 1955 when the railway line and roadway were finished at a total cost of $22 million. This was done without the preparation of any impact statement. The resulting ice-free, deep-water port on the south side of the causeway and concurrent industrialization there provided great benefits to the region.

Ship traffic transits Canso Strait through the Canso Canal which is located at the eastern end of the causeway. A 94 m swing bridge carries the road and railway line across the canal.

2. 2019 FIELD PROGRAM

From July to November 2019 instrumentation was deployed on two bottom-mounted frames and on two separate taut-wire moorings with sub-surface floats, one set on each side of the causeway (Figure 2). Barometric pressure recorders were deployed in the nearby Canal Operations Building.

2.1 CURRENT METERS

Two Acoustic Doppler Current Profilers (ADCP) were deployed, one on each side of the Causeway. The instruments were RDI 1200kHz Workhorses, bottom-mounted in frames, both in approximately 14m of water. The instruments were located approximately 500m from the Canal entrances on each side. The bin size was 0.5m. Both instruments were equipped with pressure and temperature sensors. The instrument on the north side of the Causeway ran from July 8th, 2019 until September 30th, 2019 when it inexplicably stopped. The instrument on the south side of the Causeway ran from July 8th, 2019 through recovery on November 14th, 2019 (Figures 3-6).

2.2 T/C CHAINS

Two moorings fitted with Vemco Minilog Thermographs at various depths and a single MicroCAT Temperature-Conductivity Logger each were moored near the ADCP frames (Figure 2). The MicroCATs also logged pressure (Figures 7-12). All instruments performed well except for the Southern MicroCAT where the conductivity sensor was apparently blocked for approximately the first month of the record.

2.3 CTD

CTD Casts were obtained near the positions of each of the T/C Chains both on deployment and recovery using a Seabird SBE25 CTD (Figures 13-16).

2.4 WAVE GAUGES

A RBRduet Wave Gauge (Richard Brancker Research) was mounted on each ADCP frame. Significant Wave Height (the average height of the highest one-third of all waves) from each of these instruments is shown in Figure 17. The southern wave gauge produced erroneous data during the middle portion of the record.

2.5 METEOROLOGICAL DATA

Hourly meteorological data for the mooring deployment period from Tracadie, Nova Scotia (Figure 1) was downloaded from the Environment Canada Website. A weather station at Port Hawkesbury is closer to the causeway but initial analysis suggested that wind data from this

site was not representative of conditions in Canso Strait likely due to the orographic effects of the rugged terrain characteristic of the area (Figure 18).

2.6 BAROMETRIC PRESSURE AND WATER LEVEL

A HOBO pressure recorder was deployed on each bottom frame and two HOBO pressure recorders were deployed at the Canal Operations Centre to measure barometric pressure.

2.7 CANAL OPERATION

A subset of the log of vessel passages through the Canso Canal containing only the dates, times and direction of passage for the years 2016-2019 was obtained from the Canadian Coast Guard Marine Security Operations Centre (Figure 19-20).

3. ANALYSIS AND INTERPRETATION

The Canso Causeway separates two quite different oceanographic regimes. In summer, the Southern Gulf of Saint Lawrence is much warmer and fresher than the Eastern Scotian Shelf due to the stratifying effect of the discharge from the St. Lawrence River and the reduced depths over the Magdalen Shallows. In winter, the Southern Gulf is ice-covered. In contrast, the inshore Eastern Scotian Shelf can experience wind-driven upwelling events which can bring colder, saltier water to the surface during summer (Petrie et al 1987). In winter, there is no significant ice cover. The tides in the Southern Gulf are mixed diurnal/semi-diurnal and are smaller than those of the Eastern Scotian Shelf, which are mainly semi-diurnal.

3.1 CURRENTS

Currents near the Causeway are generally small as would be expected near what is effectively the end of a closed channel. Practical considerations prevented locating the current meters near the canal entrances so as not to interfere with the passage of shipping. As a result of this and the relatively small water volumes released during normal locking activities, the instruments did not register any currents which could be attributed to canal operation.

3.1.1 North of the Causeway

As shown in Figure 4, on the north side of the causeway the ADCP recorded relatively large currents on the ebb tide in a direction at almost right angles to the channel axis. This is a result of the location of the instrument mooring directly off the mouth of Long Pond, a barachois (Figure 21). The outflow from this body of water on the ebb would occur as a jet as opposed to the inflow, which would be more diffuse, leading to the observed asymmetry in the observed currents over the tidal cycle. Although difficult to separate from the effect of the proximity of the instrumentation to Long Pond, there is some indication of intermittent two-layer flow parallel to the channel axis, probably wind-driven.

3.1.2 South of the Causeway

Observed currents on the south side of the causeway are much smaller than those observed on the north side and are generally parallel to the channel axis (Figures 5-6). As on the north side, there is some indication of intermittent two-layer flow parallel to the channel axis, again probably wind-driven.

3.2 TEMPERATURE AND SALINITY

3.2.1 North of the Causeway

Figure 7 shows a contour plot of the vertical temperature distribution from the northern T-Chain for July through September 2019. Apparent is strong vertical stratification with a mixed layer depth of approximately 10m. This is also apparent in Figure 13. Figure 11 shows data recorded by the MicroCAT on this mooring. Four significant events are apparent: an intrusion of colder water on July 12-14, an intrusion of colder water near August 8th, an intrusion of much warmer water near August 12th and a complete breakdown of stratification on September 7-8th. The first event can be associated with an interval of persistent S to SE winds observed at Tracadie (not shown). The second event is related to the passage of a weather disturbance followed by a period of persistent southerly winds. The third appears to be related to an interval of persistent westerly winds. The passage of Hurricane Dorian over September 7-8 resulted in a complete breakdown of vertical stratification followed by gradual vernal cooling where vertical stability was maintained by the fresher surface water (Figure 8, Figure 14).

3.2.2 South of the Causeway

Figure 9 shows a contour plot of the vertical temperature distribution from the southern T-Chain for July through September 2019. The southern side is seen to be much cooler and saltier than the northern side and with less stratification (Figure 12). This is also shown in Figure 15 where the increased salinity is also apparent. Many intrusions of colder bottom water are apparent, most likely due to upwelling events on the Scotian Shelf (Petrie et al. 1987). On the south side as well, the passage of Hurricane Dorian resulted in a breakdown of vertical stratification. This is followed by gradual vernal cooling.

3.3 WAVES

3.3.1 North of the Causeway

The northern approaches to the Canso Causeway, which open directly onto Saint Georges Bay and the Southern Gulf of Saint Lawrence, are much more exposed than the southern approaches. The results of this are readily apparent in the plots of significant wave height shown in Figure 17. (The significant wave height is the average height of the highest one-third of all waves measured which is roughly equivalent to the estimate that would be made by a visual observer). Figure 22 shows the component of wind speed along the axis of the causeway observed at Tracadie Nova Scotia and the Significant Wave Height on the North side of the Causeway. Events with significant wave heights of over 0.1m are seen to be associated with wind speeds along the channel axis toward the causeway greater than about 5 m/s. Winds observed at the Port Hawkesbury weather station, which is closer to the causeway were found to be generally unrelated to the observed wave statistics. This is probably because of the rugged nature of the local terrain. One notable exception to the

observed relationship between the wind and the wave height is the wave event near the 9th of September. This was during the passage of Hurricane Dorian when waves generated further out in the Gulf of Saint Lawrence probably propagated in the region.

3.3.2 South of the Causeway

The southern approaches to the causeway are longer and more convoluted and open onto Chedabucto Bay rather than directly onto the Scotian Shelf. The result is little wave activity on the southern side as shown in Figure 17.

3.4 WATER LEVELS

The tides of Saint Georges Bay, on the north side of the Causeway (Figure 4), show a marked diurnal inequality, which is similar to the tide at Charlottetown. This is quite different from the tides in Chedabucto Bay, on the south side of the Causeway (Figure 6), which is similar to the Atlantic tide at Halifax. The maximum range of the tide in Saint Georges Bay is approximately 1.5m, whereas in Chedabucto Bay it is approximately 2.0m (Fothergill et al 1955). Before Causeway construction, this difference in the tidal regimes produced a varying hydraulic head between the two ends of the Strait, setting up powerful tidal currents. There was a slight slope to the mean surface, downwards from Saint Georges Bay to the Atlantic Ocean, giving rise to an appreciable net flow southward through the Strait. This slope in mean level, formerly spread throughout the Strait, is now recorded as an abrupt change in level on either side of the Causeway (Trites 1979). The long-term average difference in level across the causeway is between 6cm, (Lawrence and Greenberg 1979) and 9cm (Fothergill et al. 1955).

Several of the instruments deployed on each side of the causeway were equipped with pressure sensors. Analysis was focused on the time series produced by the two MicroCATs as these instruments ran properly for the whole deployment period and are noted for their high-quality pressure sensors. The northern instrument sampled at 10 minute intervals while the southern instrument sampled at 1 minute. The data from the southern instrument was down sampled to 10 minutes to allow computation of the level difference across the causeway.

3.4.1 North of the Causeway

Figure 23 shows the results of a tidal analysis of the water level on the North side of the Causeway as measured by the MicroCAT (Pawlowicz et al. 2006). Table 1 shows the amplitude and phase of the five largest fitted constituents. The two diurnal constituents O1 and K1 are seen to be the largest after the main lunar semi-diurnal constituent M2 leading to the large diurnal inequality mentioned earlier. The fitted tides account for 82.0% of the total variance in the record. Note that this record has not been corrected for the effect of variations in atmospheric pressure on the calculation of water level from the MicroCAT pressure channel. The passage of Hurricane Dorian September 7th- 8th is apparent in the residual

record. Figure 24 shows the power spectra of the residual after the tidal signal is removed. The large low frequency peak is most likely due to variations in barometric pressure. The smaller high frequency peaks are probably related to the barotropic seiche periods of Saint Georges Bay (estimated at 117 minutes) and the northern arm of Canso Strait (estimated at 33 minutes) (Rueda and Schladow 2002). None of these are energetic enough to be relevant to the present study.

3.4.2 South of the Causeway

Figure 25 shows the results of a tidal analysis of the water level on the South side of the Causeway as measured by the MicroCAT. Table 2 shows the amplitude and phase of the five largest fitted constituents. The top three constituents are semi-diurnal followed by a much smaller diurnal constituent. The fitted tides accounted for 95.3% of the total variance in the record. Note that this record has not been corrected for variations in atmospheric pressure either. Apparent in the residual record is the even larger response to Hurricane Dorian. Figure 26 shows the power spectra of the residual after the tidal signal is removed. The low frequency peak due to atmospheric pressure variations is present but not as pronounced as that in the northern record. The peaks at periods of approximately 12, 8 and 4 hours have no obvious cause but may be related to phenomena in Chedabucto Bay (Barber and Taylor 1977) and on the Scotian Shelf. The tiny peak at a period of approximately 1 hour is hear the estimated barotropic seiche period of 51 minutes for the southern arm of the Strait. Again, none of these are energetic enough to be relevant to the present study.

3.4.3 Cross Causeway Difference

To calculate the water exchanged in each lock operation it is necessary to know the difference in water level from one side to the other. To allow the calculation of predicted water level differences across the causeway at times other than the instrument deployment period a tidal analysis was performed on the difference between the pressure channels from the north and south MicroCATs. The mean was removed from each record. Figure 27 shows the results. The analysis accounted for 85.3% of the variance in the record. Table 3 shows the amplitude and phase of the five largest fitted constituents. A positive level difference means the north side is higher leading to a potential southward transport. Note that this calculated level difference is independent of the correction of the instrument pressure channel for changes in atmospheric pressure which would be expected to be the same for both records. The maximum observed level difference including the estimated mean difference of 7cm was 1.52m at 0050 local time on September 8th, 2019. The minimum observed difference was -1.21m at 1550 local time on September 7th, 2019. Both of these are obviously related to the passage of Hurricane Dorian. The cross-causeway level difference is seen to exhibit a significant diurnal inequality. At the peak of spring tides, the largest level difference of the day can reach +/- 1m. The smaller difference of the day is typically +/- 0.5m. During Neap tides, the diurnal inequality is less pronounced and is typically less than +/- 0.5m.

3.5 LOCK OPERATION

The Canso Lock is located at the east end of the Causeway. The lock is 24.4m wide by 250m long. The lock is normally in operation from April through December of each year. Ships with a draught of not more than 8.8m and a length of not more than 224m may proceed through the lock 7 days a week 24 hours a day during the navigation season. Ships with a draught of not more than 9.1m may proceed through the lock when tidal conditions are favourable (Canadian Hydrographic Service 1990). Table 3 shows the average number of locking events by month and year. The table shows 'locking events' which often involve more than one small vessel transiting the lock at the same time. In 2016 the lock was closed November-December and did not open again until May 2017. These months are not included in the calculations of the monthly averages and years 2016 and 2017 are not included in the calculation of the yearly averages. There are typically around 500 events in each direction each year. The most active months are July and August with slightly more than 100 locking events in each direction each month.

4. DISCUSSION AND CONCLUSIONS

Three mechanisms might be postulated to lead to the transport of water and any related pathogens across the causeway: 1) Percolation through the rock fill from which the causeway is constructed. 2) Over-topping of the causeway by wave action during storm events 3) Water passed as part of Canso Canal locking operations. Each of these is discussed below.

4.1 PERCOLATION

Given the relatively small level differences from one side to the other of what is essentially an earthen dam (approximately +/- 1m) this mechanism is not expected to result in any significant transport of water through the causeway. Over the last 50+ years suspended sediments have likely been deposited in the interstitial spaces in the rock fill of which the causeway is composed resulting in a practically impervious structure.

4.2 OVER-TOPPING BY WAVES

As shown in the wave gauge observations, storm force winds from the NW can lead to significant wave action on the North side of the causeway. Assisted by the wind, breaking wave tops can transport of heavy spray across the causeway. The actual volume of water involved is difficult to estimate but is spectacular to observe and has resulted in the closure of the causeway to vehicle traffic on some occasions. Because of the strong relationship with wind speed and direction the occurrence of this phenomenon can be predicted to a certain extent.

4.3 LOCK OPERATION

The volume of water exchanged during lock operation can be estimated by making a few assumptions. If one ignores the displacement of the vessel(s) involved in the locking operation, then the volume exchanged will simply be the area of the lock multiplied by the level difference involved in a direction from high to low. This is a fair assumption as most of the transiting vessels are relatively small displacement pleasure craft and fishing vessels. Table 5 shows the pattern of water discharged during locking events for various directions of transit and initial levels in the lock. Three of the four possible scenarios result in the discharge of the volume as calculated above. Assuming that all locking events result in this discharge may thus over-estimate the exchange by 25%. Given that the volume of chronic leakage through the lock gates is an unknown, this is probably not an issue.

Figures 29 through 32 show the calculated total daily volume transport in thousands of cubic metres due to lock operation for 2018 and 2019. It is assumed that different water masses are involved in each locking operation so that northward and southward transport can occur during the same day. Figures 33 through 36 show the calculated total monthly volume transport in 10’s of thousands of cubic metres due to lock operation for 2018 and 2019. The maximum calculated total daily transports for the period 2016-2019 were 25806 m^3 to the

north on November 13th 2018 and 26431 m^3 to the south on July 17th 2019. The maximum calculated monthly totals are typically about 200,000 m^3 and occur most frequently in August.

5. ACKNOWLEDGMENTS

The assistance of Ovide J. Boudreau, Canso Strait Lock Master, who answered our many questions about lock operation and Christina P. Hunt, Lead Officer at the Canadian Coast Guard Marine Security Operations Centre, who provided data on lock operations, is gratefully acknowledged.

6. References

Canadian Hydrographic Service 1990. Sailing Directions Nova Scotia (Atlantic Coast) and Bay of Fundy. Department of Fisheries and Oceans, Ottawa, Canada.

Barber, F.G. and Taylor J. 1977. A Note on Free Oscillations of Chedabucto Bay. (MS Rep. Ser. Mar. Sci. Direct. No. 47). Marine Sciences Directorate, Department of Fisheries and the Environment.

Fothergill, N.O., Cross, C.M. and Smith, F.C.G. 1955. Tidal changes in the Strait of Canso Region. Tidal and Current Survey, Ottawa. Department of Energy, Mines and Resources, Inland Waters Branch.

Lawrence, D.J. and Greenberg, D. 1979. Estimates of pre-causeway flow through the Strait of Canso. *In* Canso Marine Environment Workshop: Part 1. Executive Summary. Part 2. an Overview. Part 3. Fishery Impacts. Part 4. Physical Oceanography and Environmental Effects. Edited by McCracken, F.D. Fisheries and Marine Service Technical Report No. 834.

Pawlowicz, R., Beardsley, B., & Lentz, S. (2006). Classical tidal harmonic analysis including error estimates in MATLAB using T_TIDE. Computers and Geosciences, 28(8), 929–937.

Petrie, B., Topliss, B. and Wright, D. 1987. Coastal upwelling and eddy development off Nova Scotia. J. Geophys. Res.29: 12979–12991

Rueda F.J. and Schladow, S.G. 2002. Surface seiches in lakes of complex geometry Limnol. Oceanogr. 47(3), 906–910

Trites, R.W. 1979. Some physical oceanographic features in relation to the Canso causeway – an overview. *In* Canso Marine Environment Workshop: Part 1. Executive Summary. Part 2. an Overview. Part 3. Fishery Impacts. Part 4. Physical Oceanography and Environmental Effects. Edited by McCracken, F.D. Fisheries and Marine Service Technical Report No. 834.

FIGURES

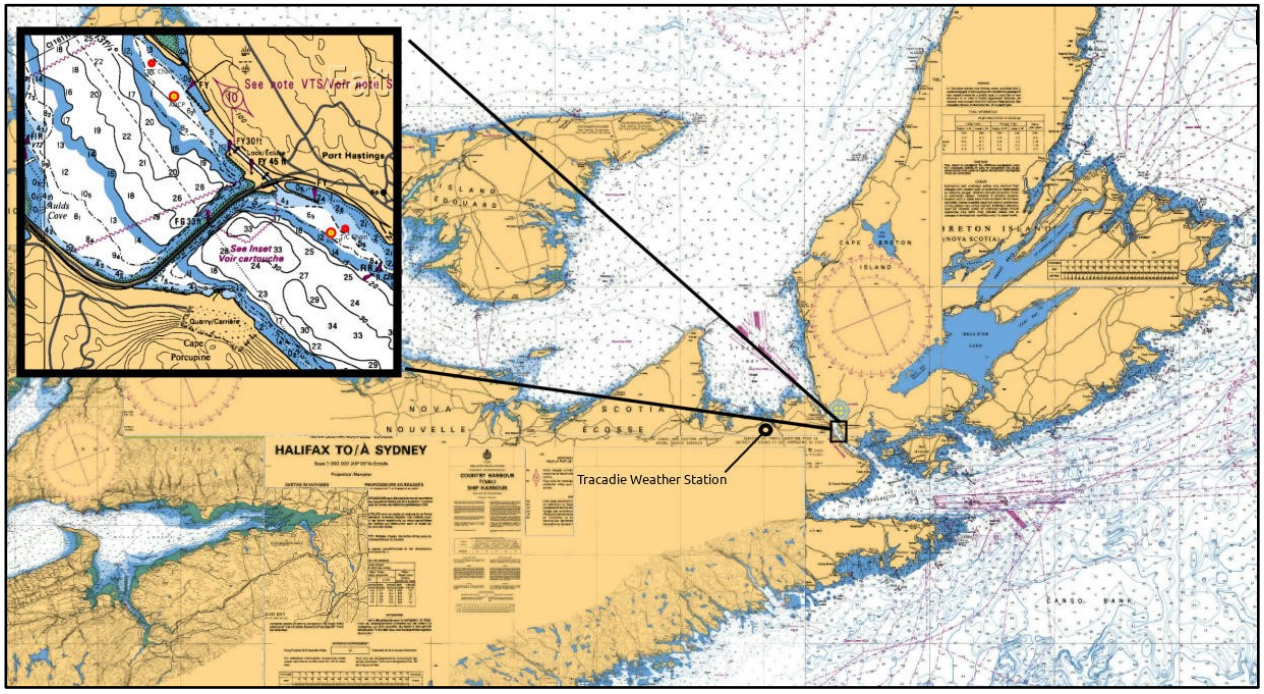

Figure 2: Map showing locations of Canso Strait and the Causeway.

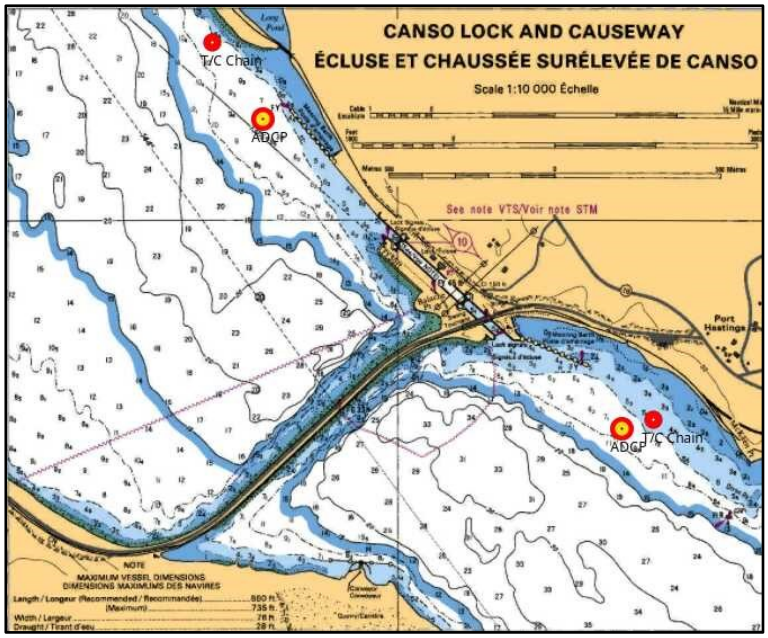

Figure 1: Map showing location of instruments deployed July through November 2019.

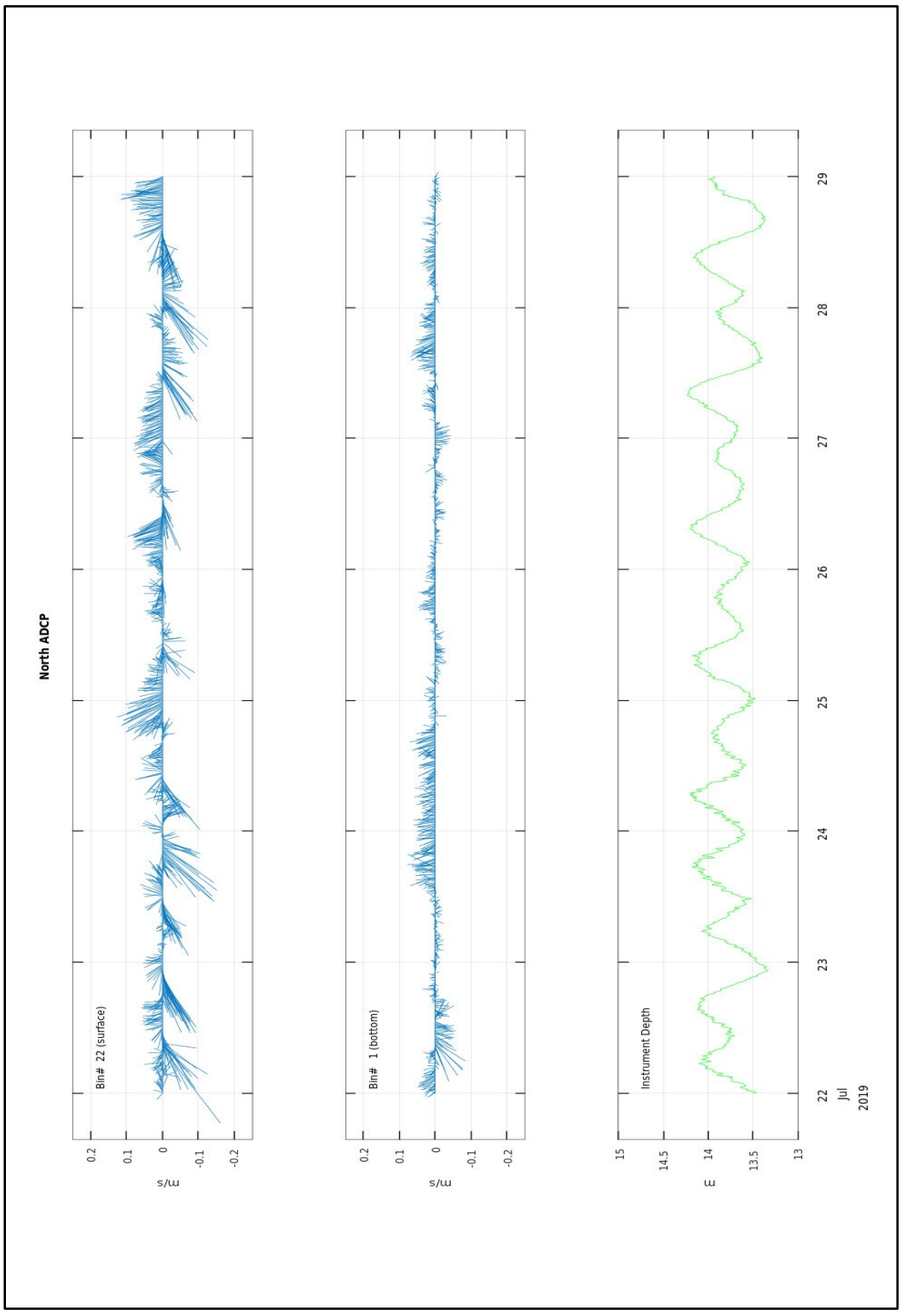

Figure 3: Surface and bottom currents from the ADCP on the North side of the Causeway during a Period of Neap Tides. Bin 1 is at an average depth of approximately 13m and bin 22 at approximately 2m.

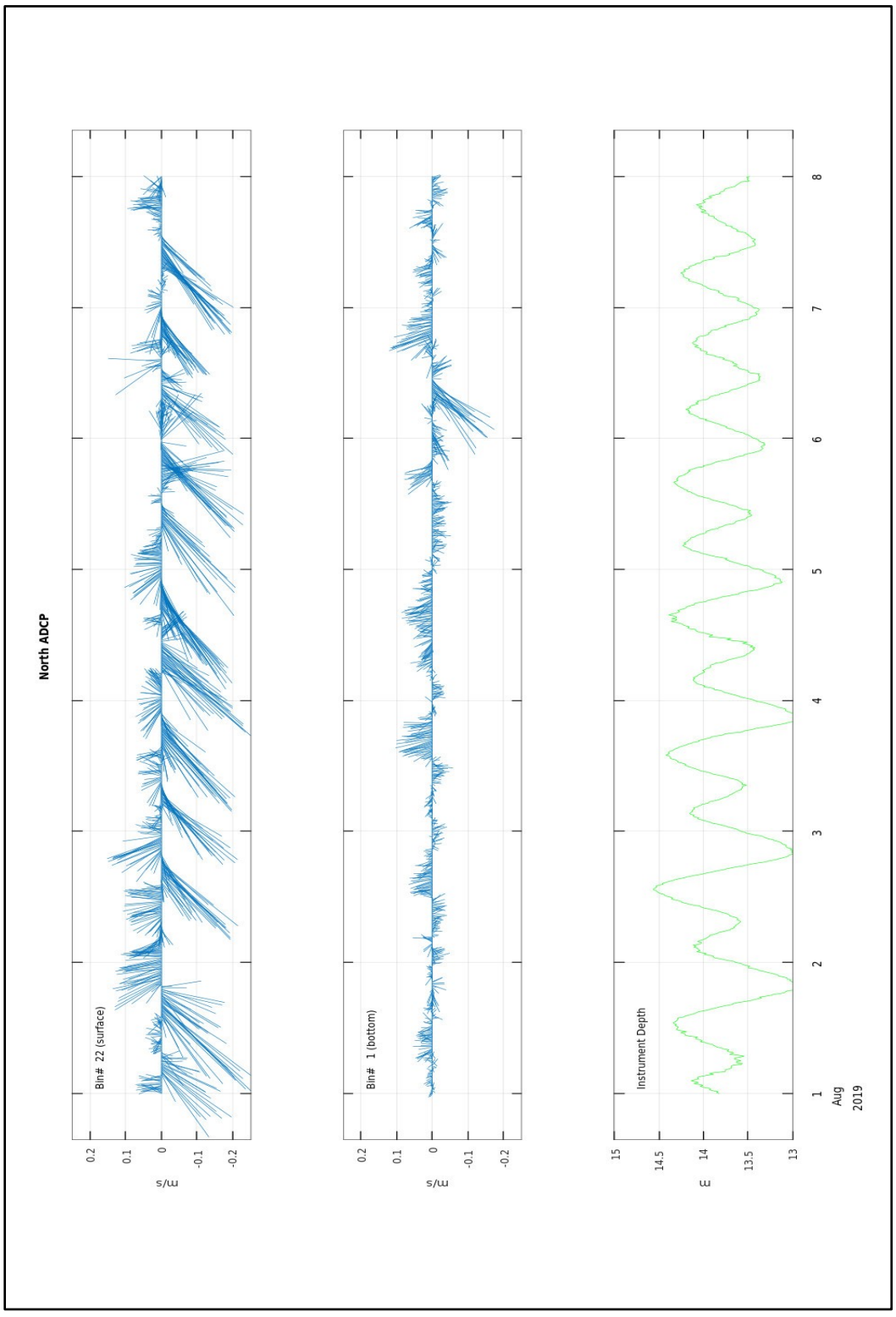

Figure 4: Surface and bottom currents from the ADCP on the North side of the Causeway during a Period of Spring Tides. Bin 1 is at an average depth of approximately 13m and bin 22 at approximately 2m.

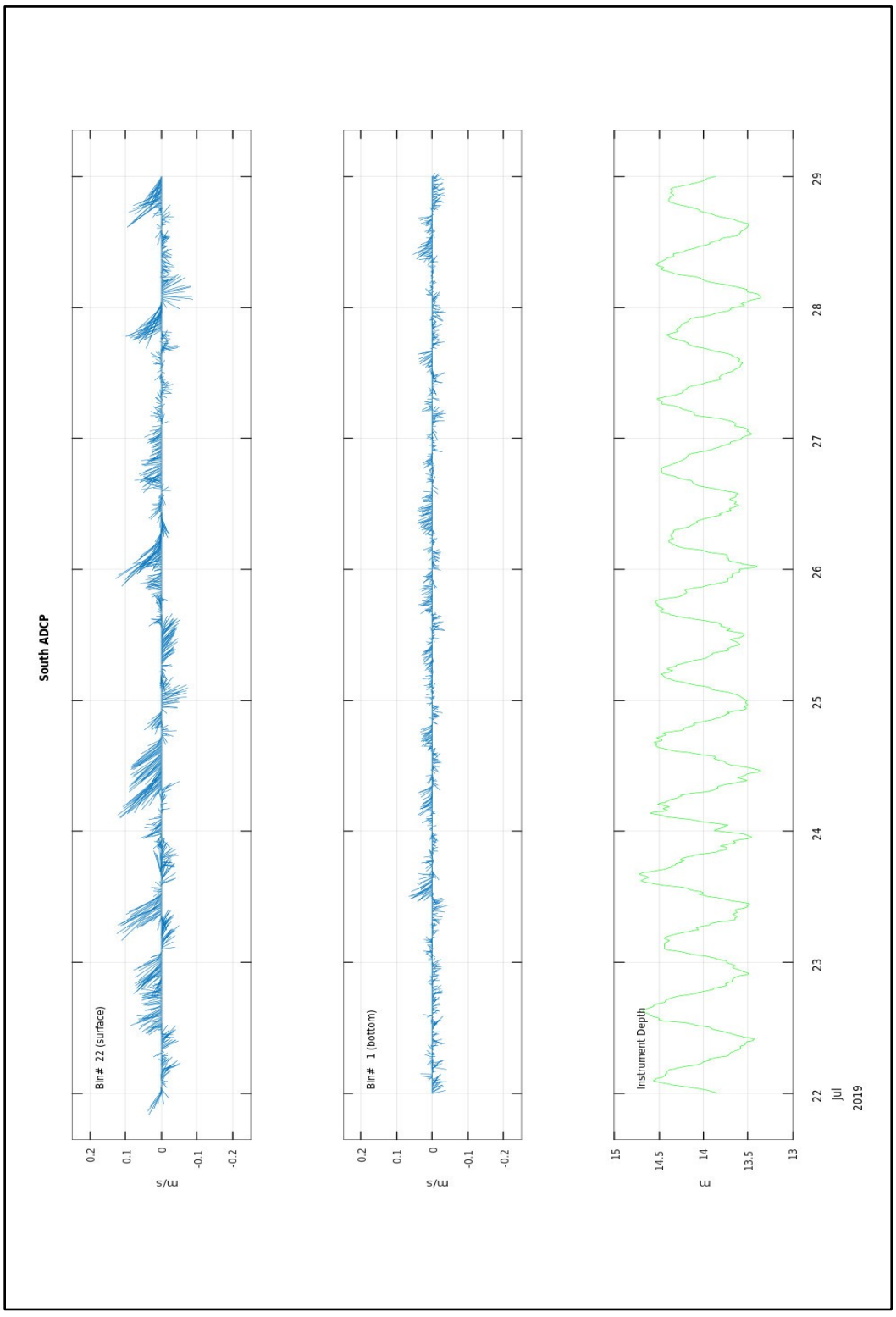

Figure 5: Surface and bottom currents from the ADCP on the South side of the Causeway during a Period of Neap Tides. Bin 1 is at an average depth of approximately 13m and bin 22 at approximately 2m.

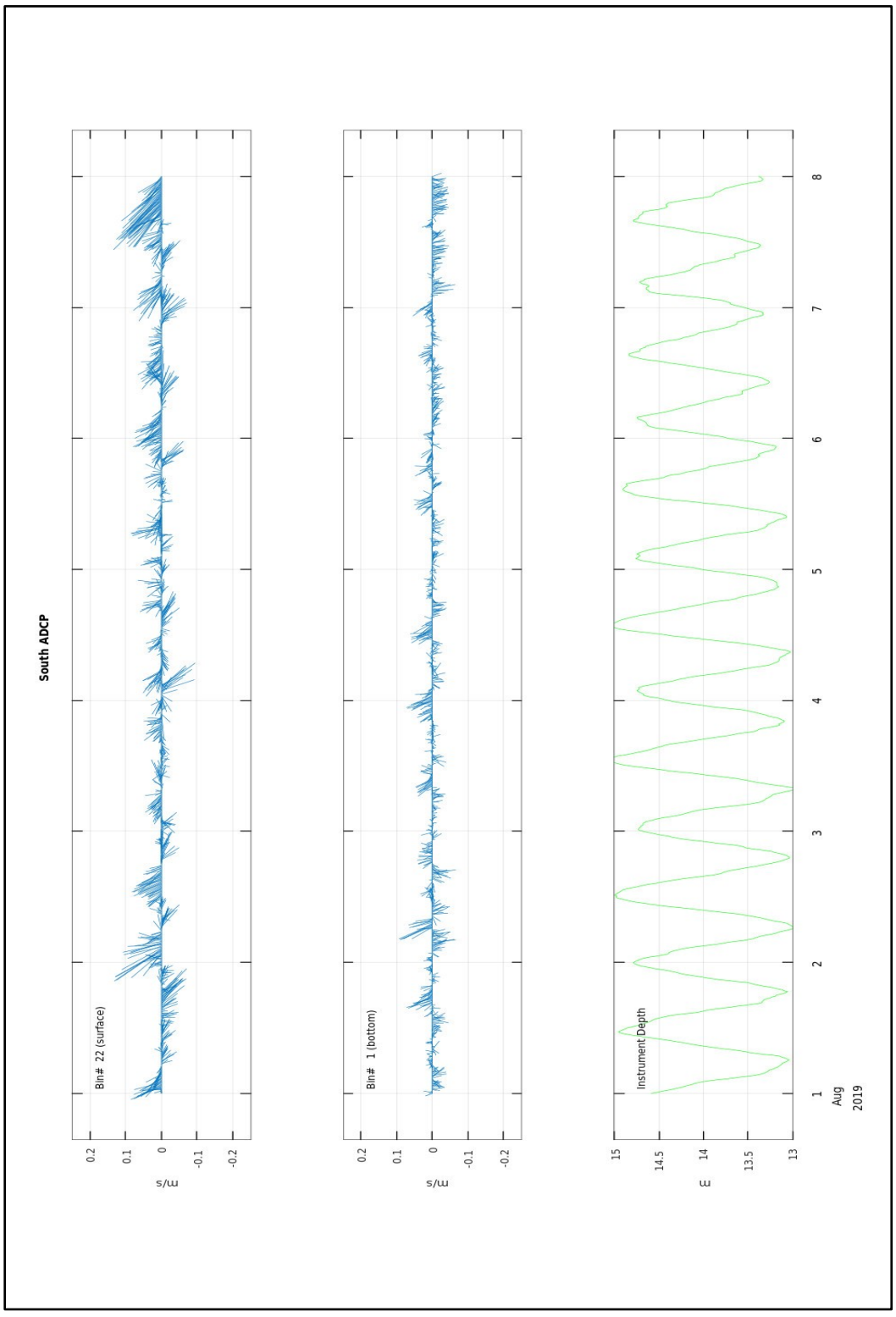

Figure 6: Surface and bottom currents from the ADCP on the South side of the Causeway during a Period of Spring Tides. Bin 1 is at an average depth of approximately 13m and bin 22 at approximately 2m.

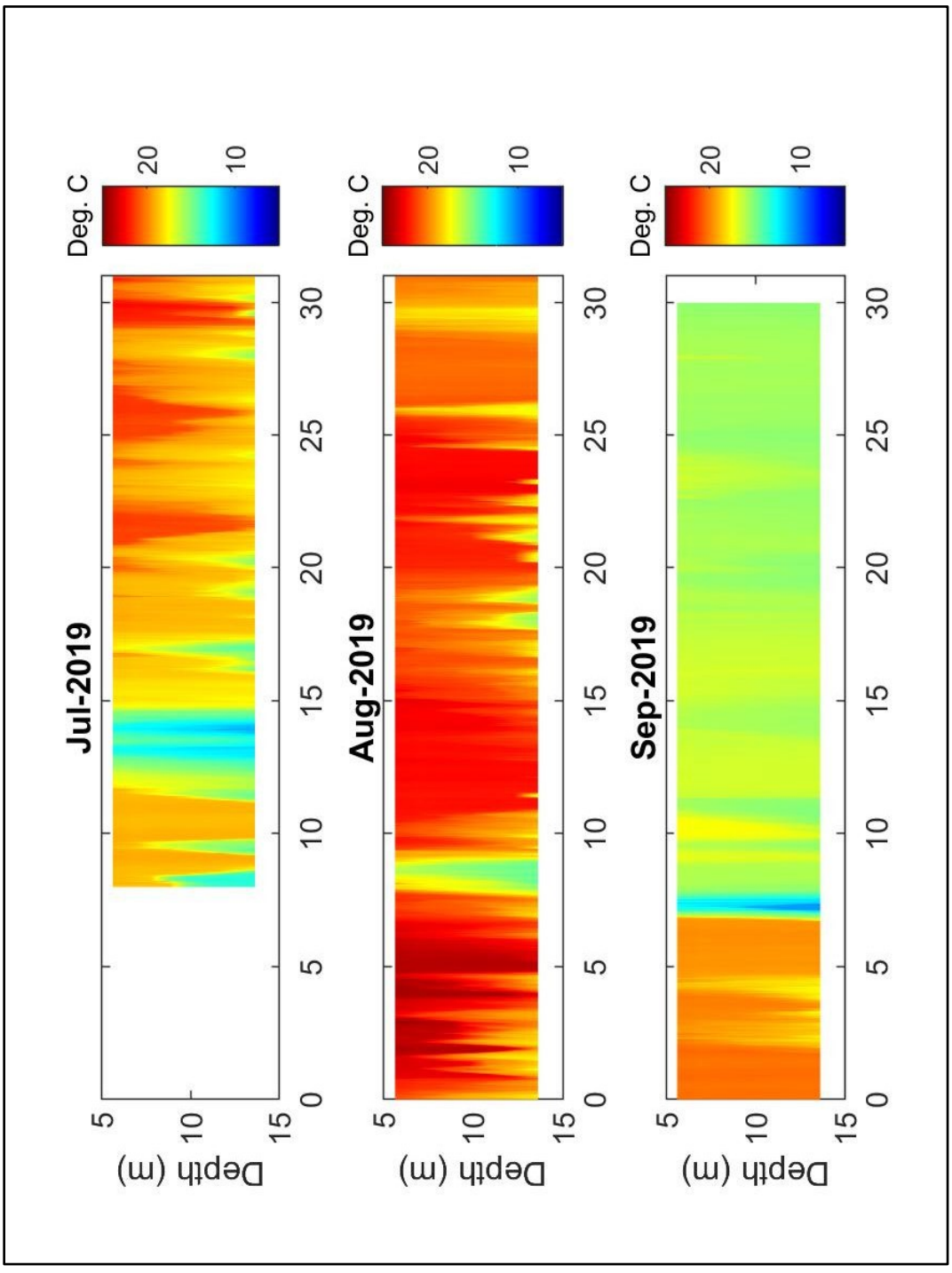

Figure 7: Contour Plot of Temperature from Northern T-Chain July – September 2019.

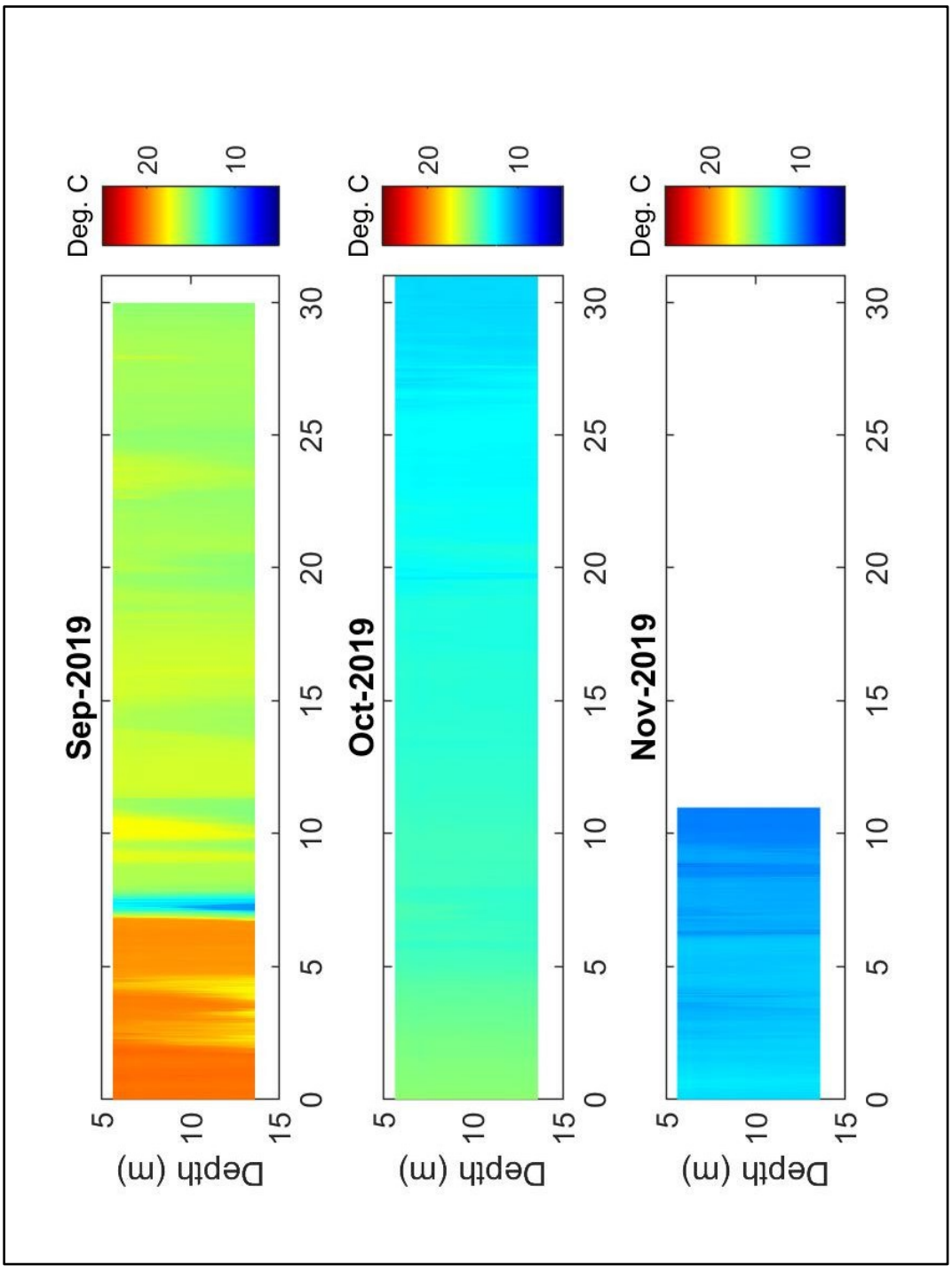

Figure 8: Contour Plot of Temperature from Northern T-Chain September - November 2019.

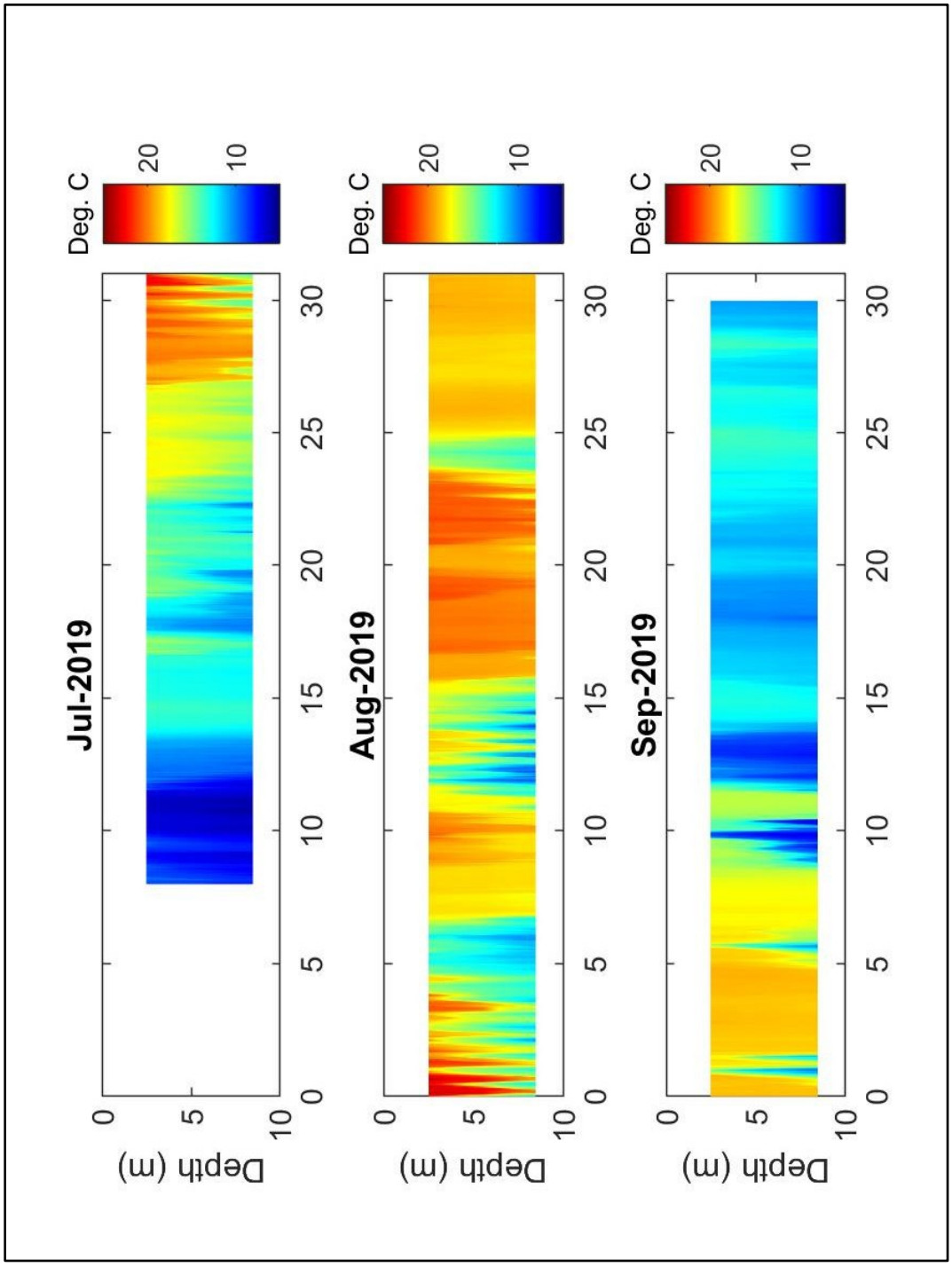

Figure 9: Contour Plot of Temperature from Southern T-Chain. July - September 2019. Note difference in depth scale from Figures 7 and 8.

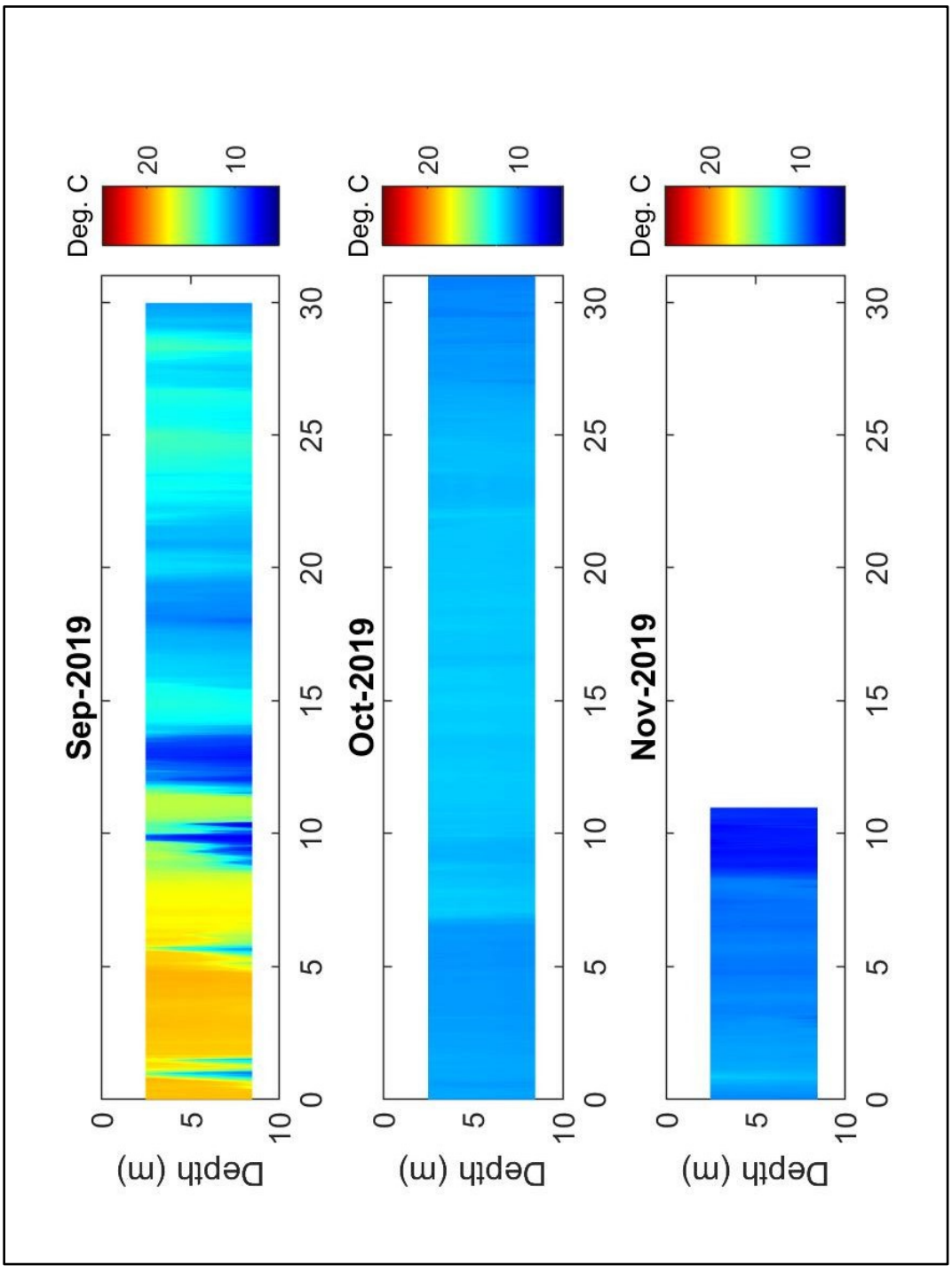

Figure 10: Contour Plot of Temperature from Southern T-Chain September - November 2019. Note difference in depth scale from Figures 7 and 8.

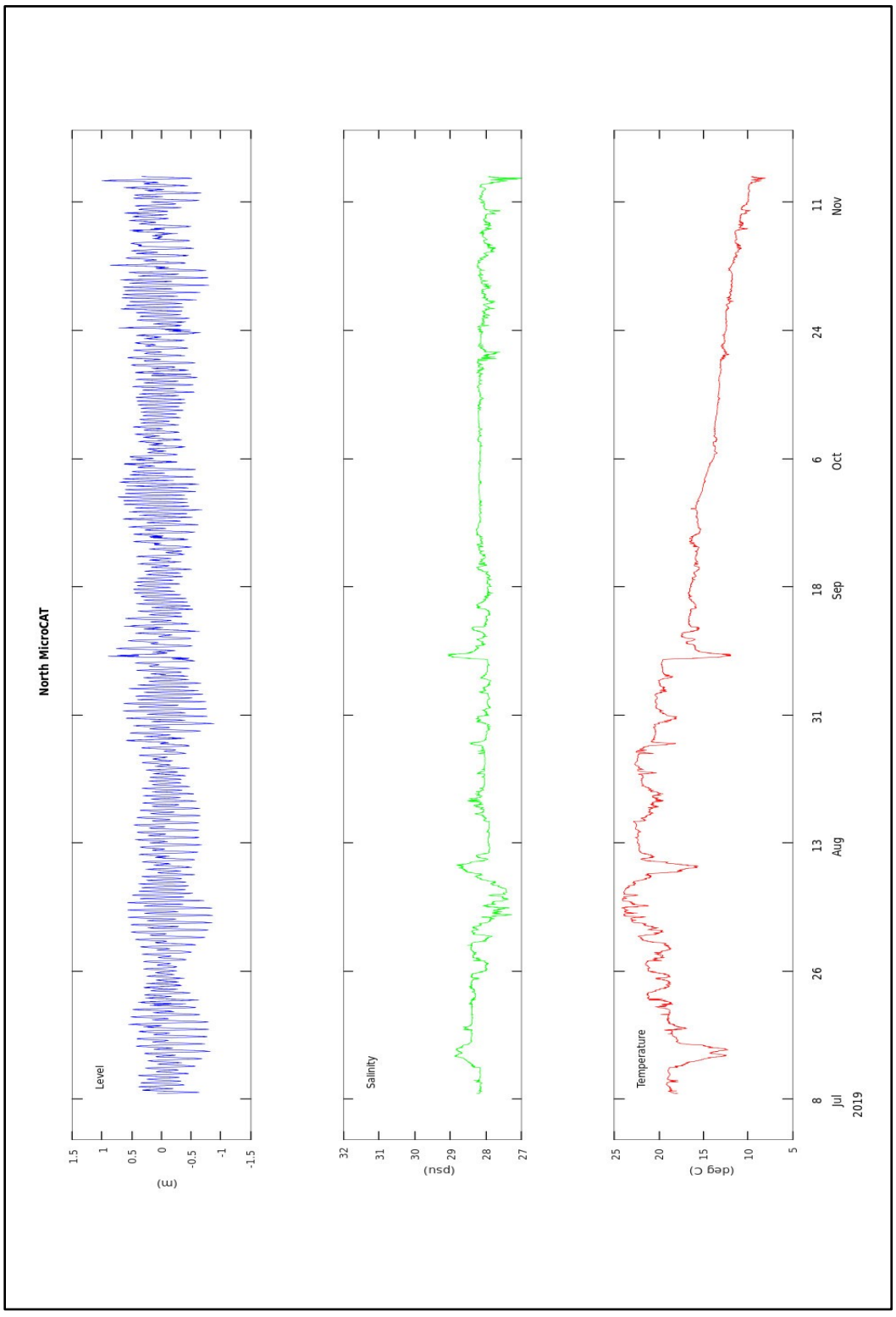

Figure 11: Plot of Data from MicroCAT mounted on Northern T-Chain.

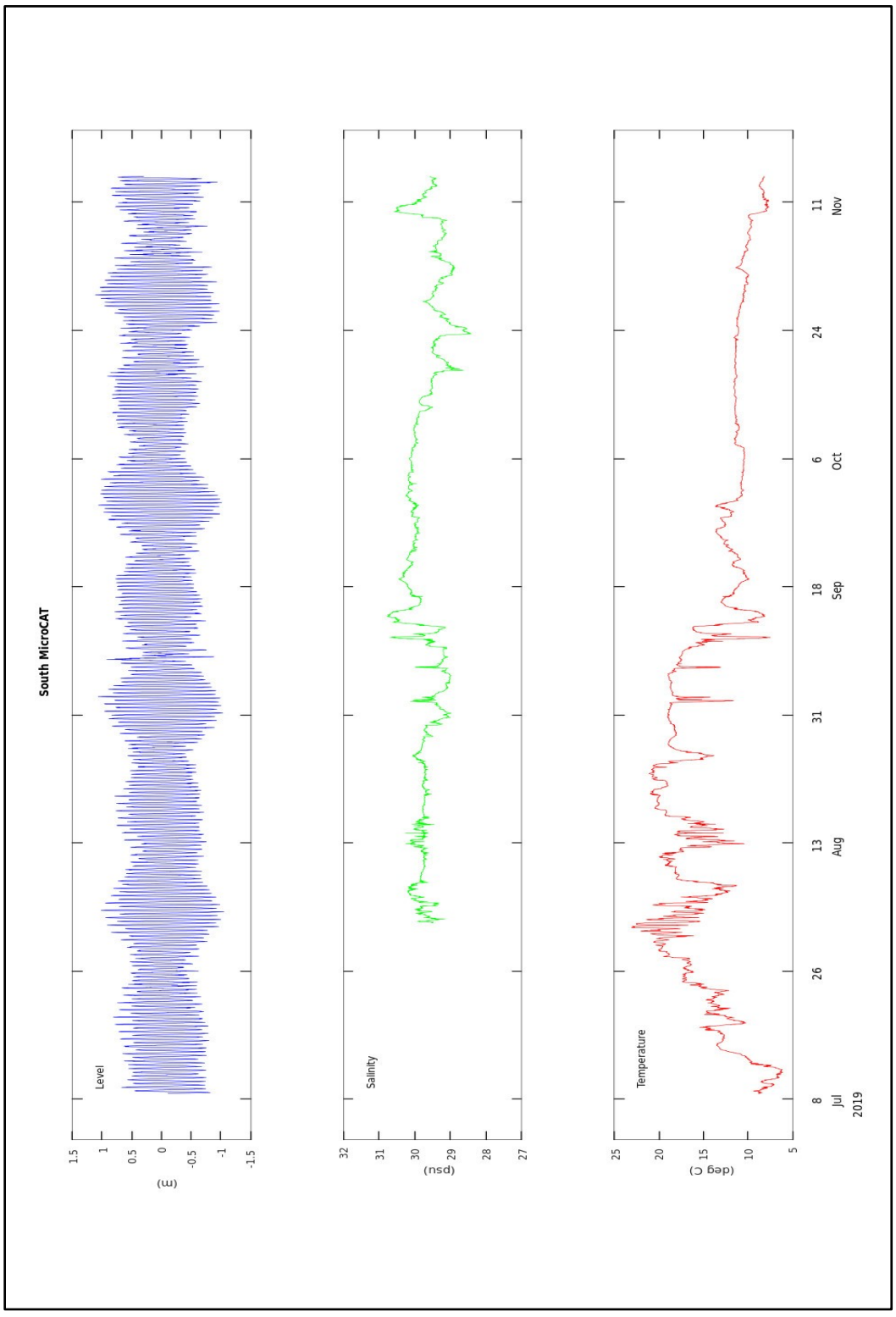

Figure 12: Plot of Data from MicroCAT mounted on Southern T-Chain.

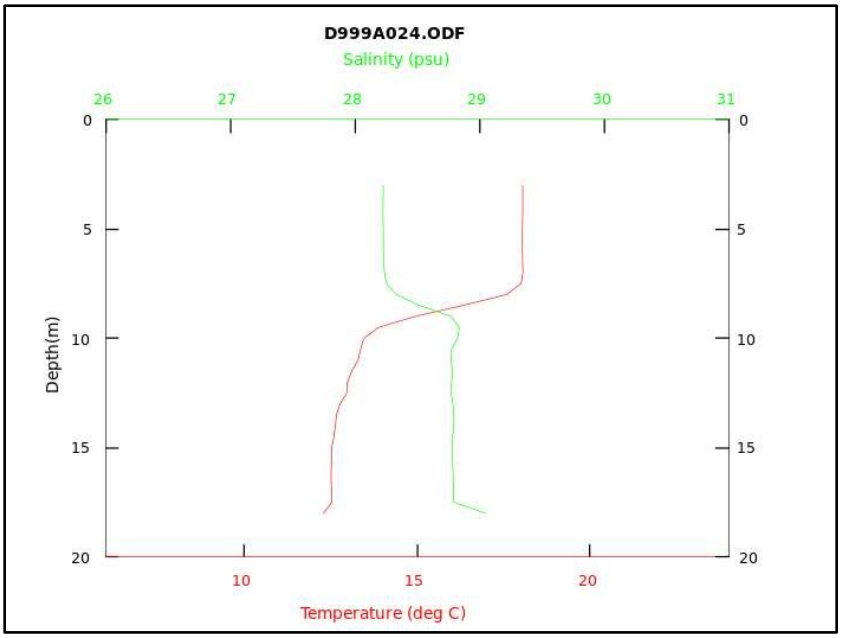

Figure 13: CTD on Deployment of Northern T-Chain July 8 2019 17:10 UTC.

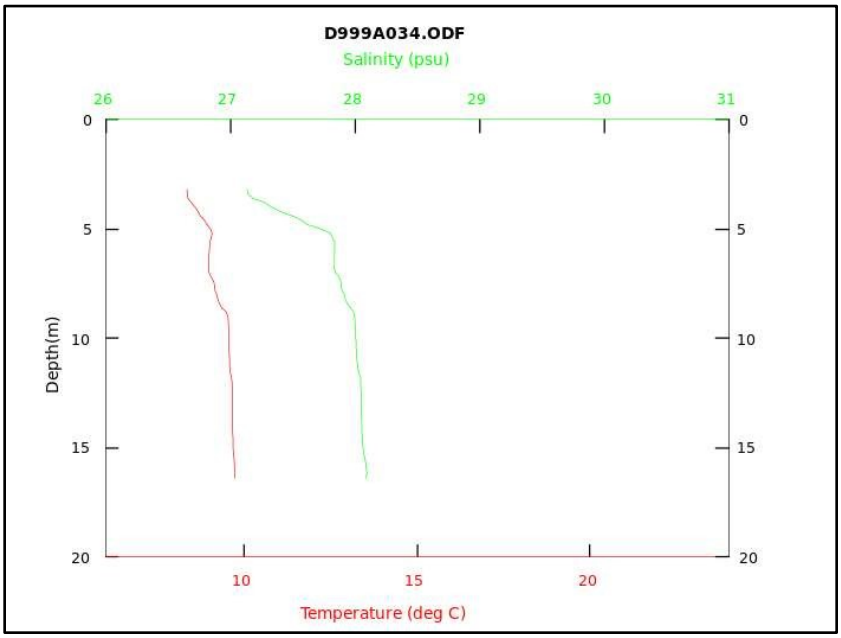

Figure 14: CTD on Recovery of Northern T-Chain November 14 2019 14:56 UTC.

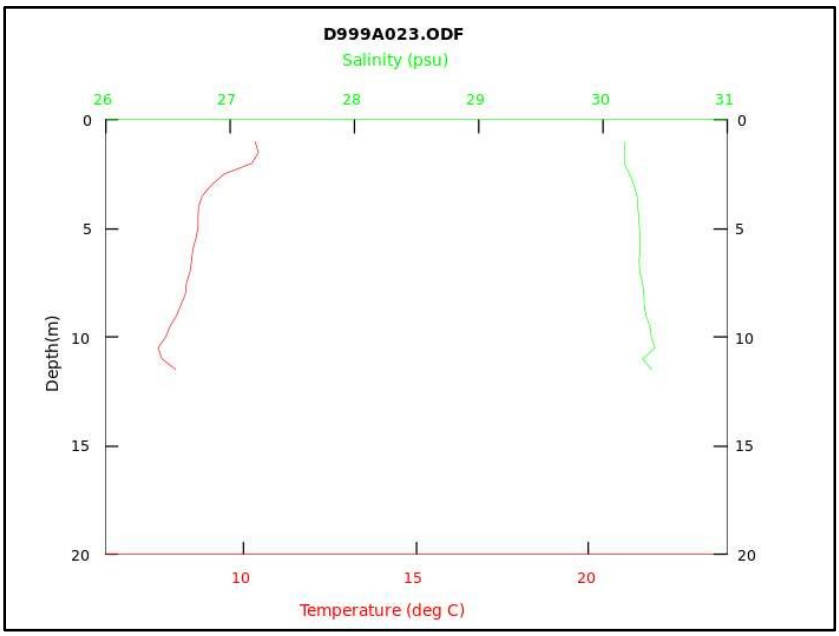

Figure 15: CTD on Deployment of Southern T-Chain July 8 2019 19:42 UTC.

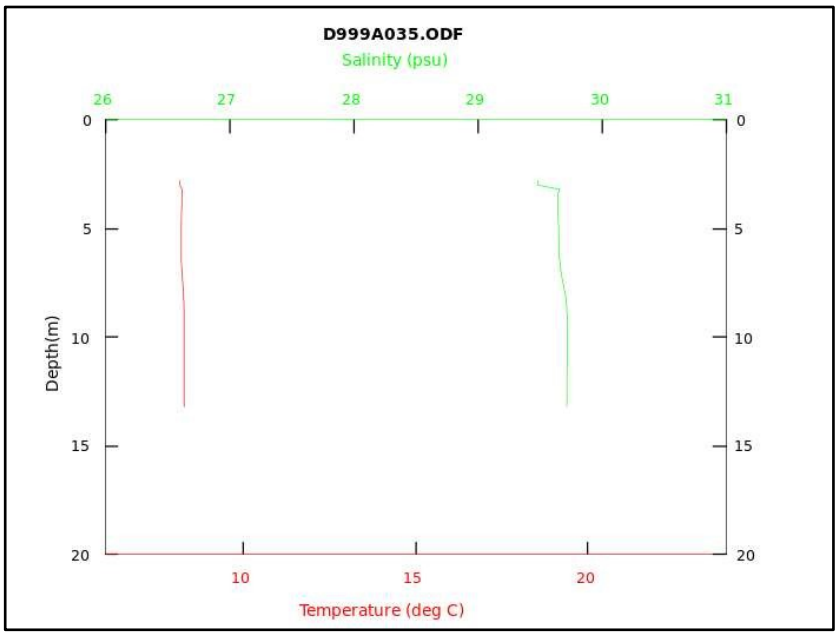

Figure 16: CTD on Recovery of Southern T-Chain November 14 2019 16:41 UTC

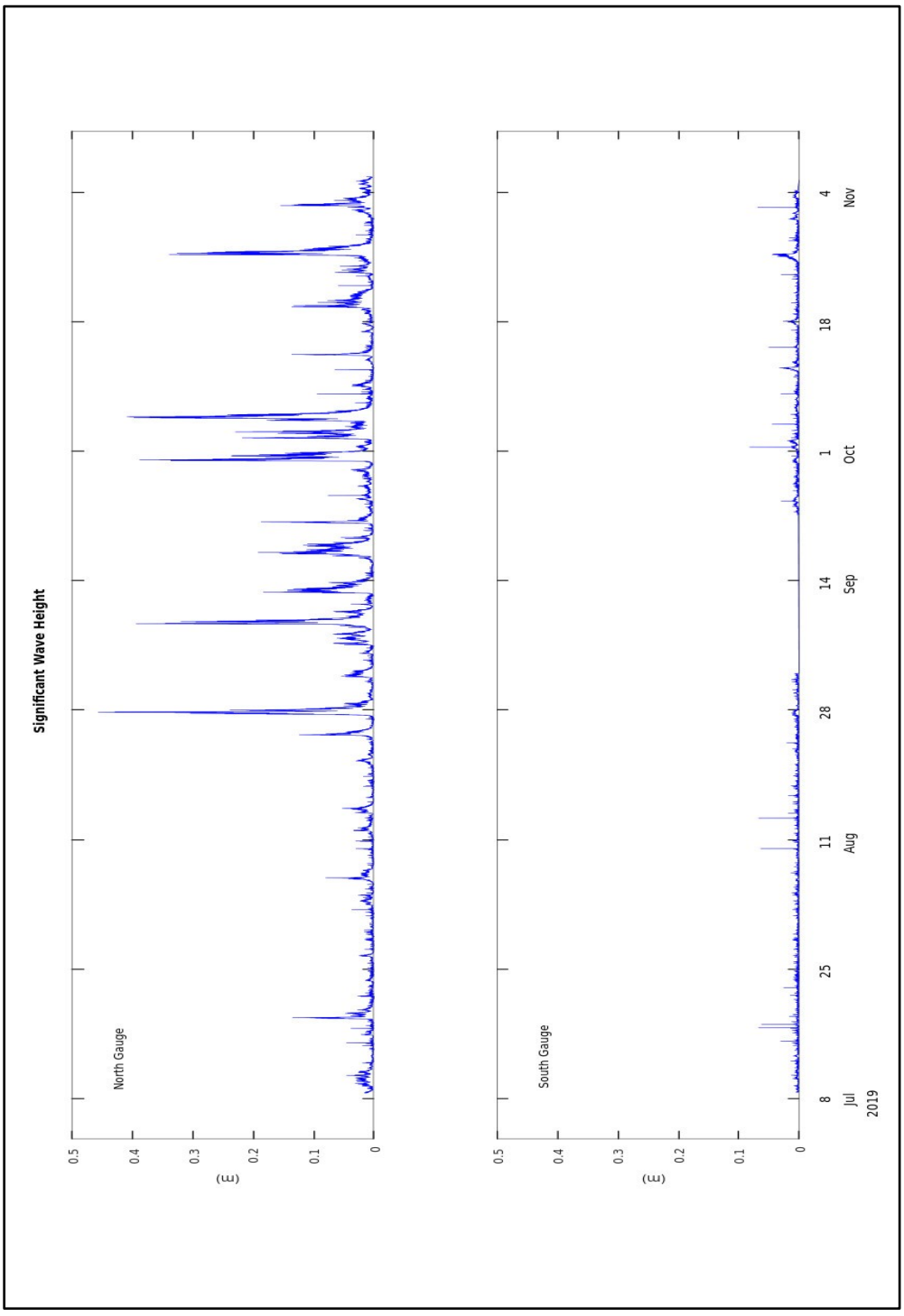

Figure 17: Significant Wave Height from gauges deployed North and South of the Causeway.

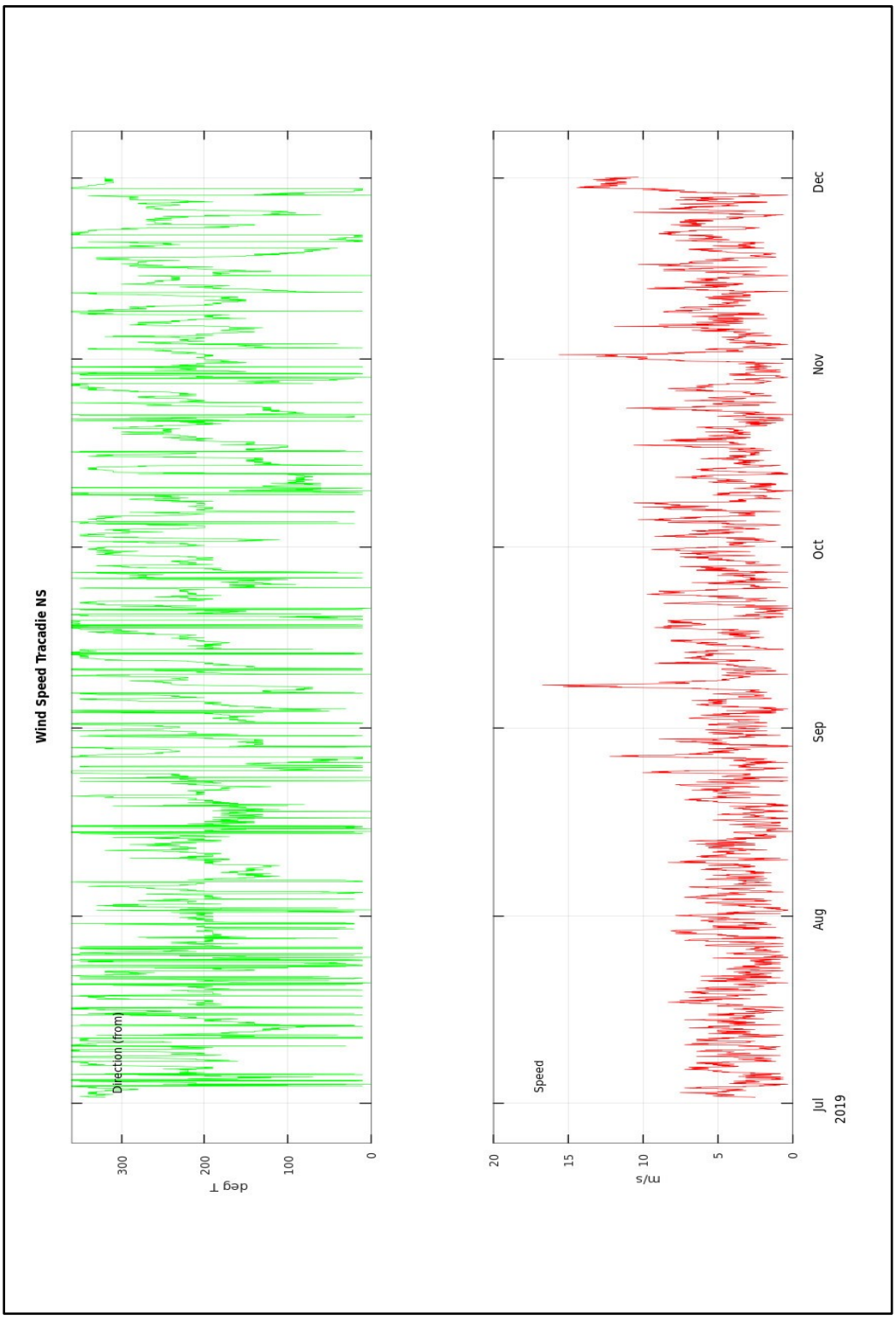

Figure 18: Wind Speed and Direction from Tracadie Weather Station.

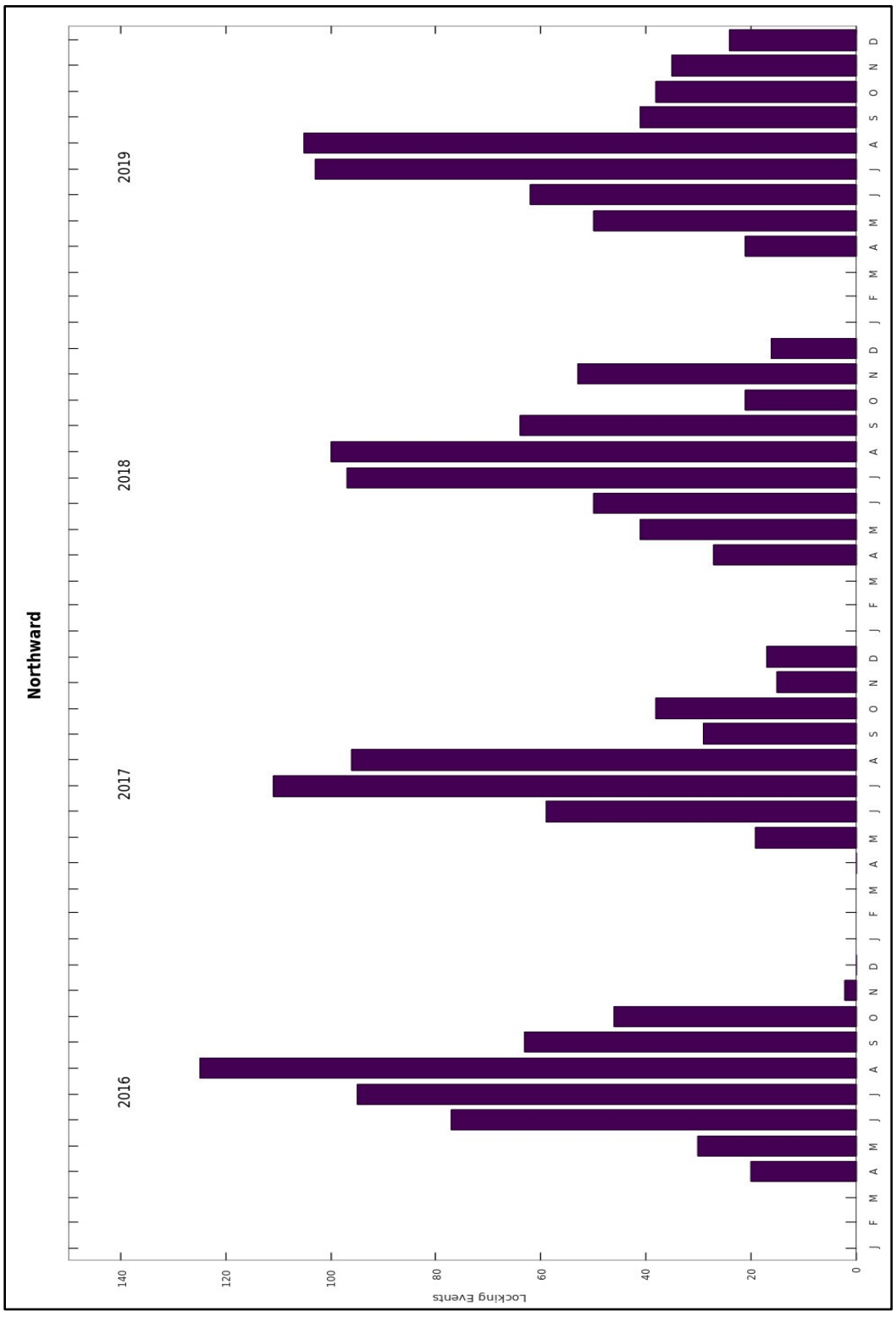

Figure 19: Count of Northward Locking Events for the Canso Canal.

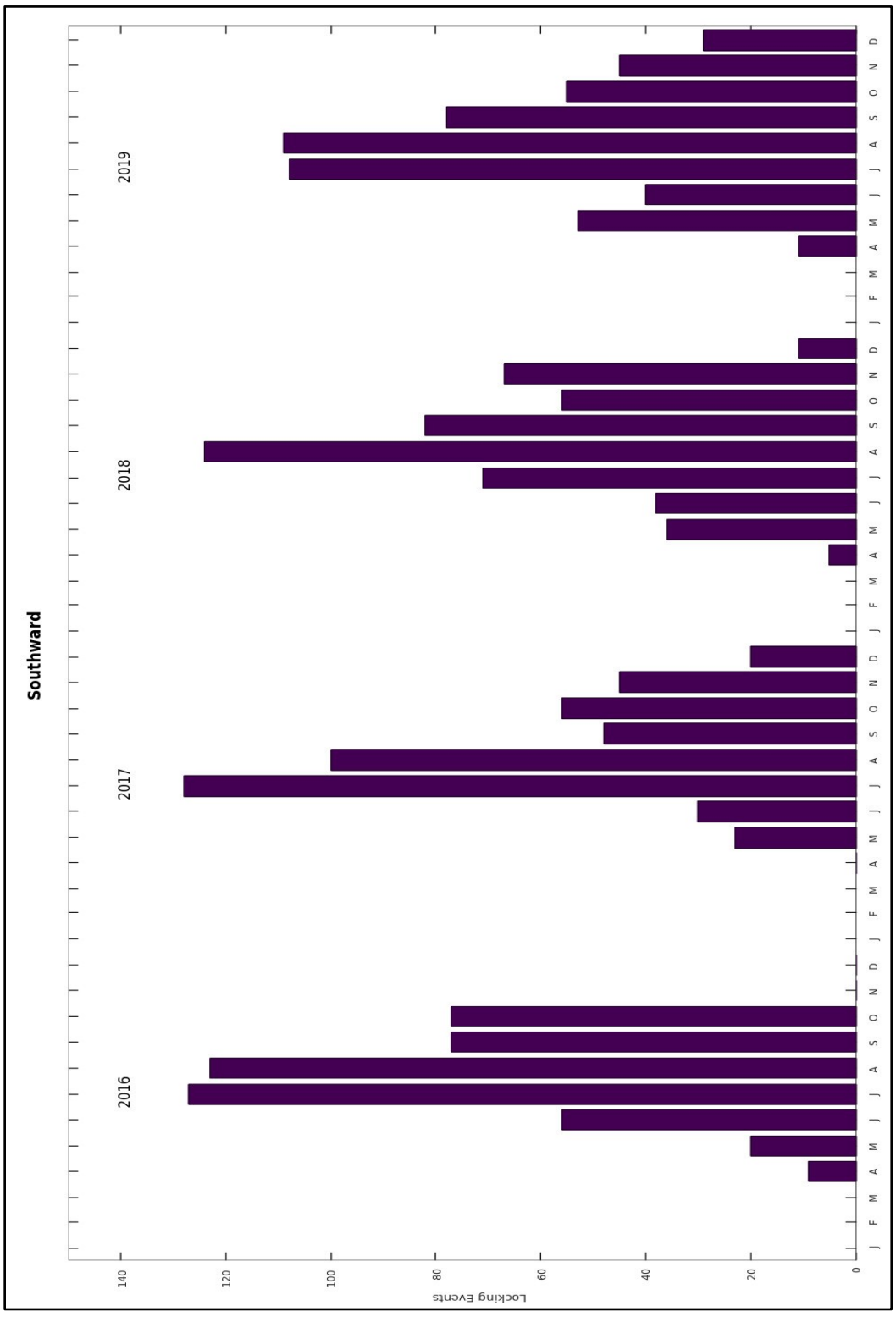

Figure 20: Count of Southward Locking Events for the Canso Canal.

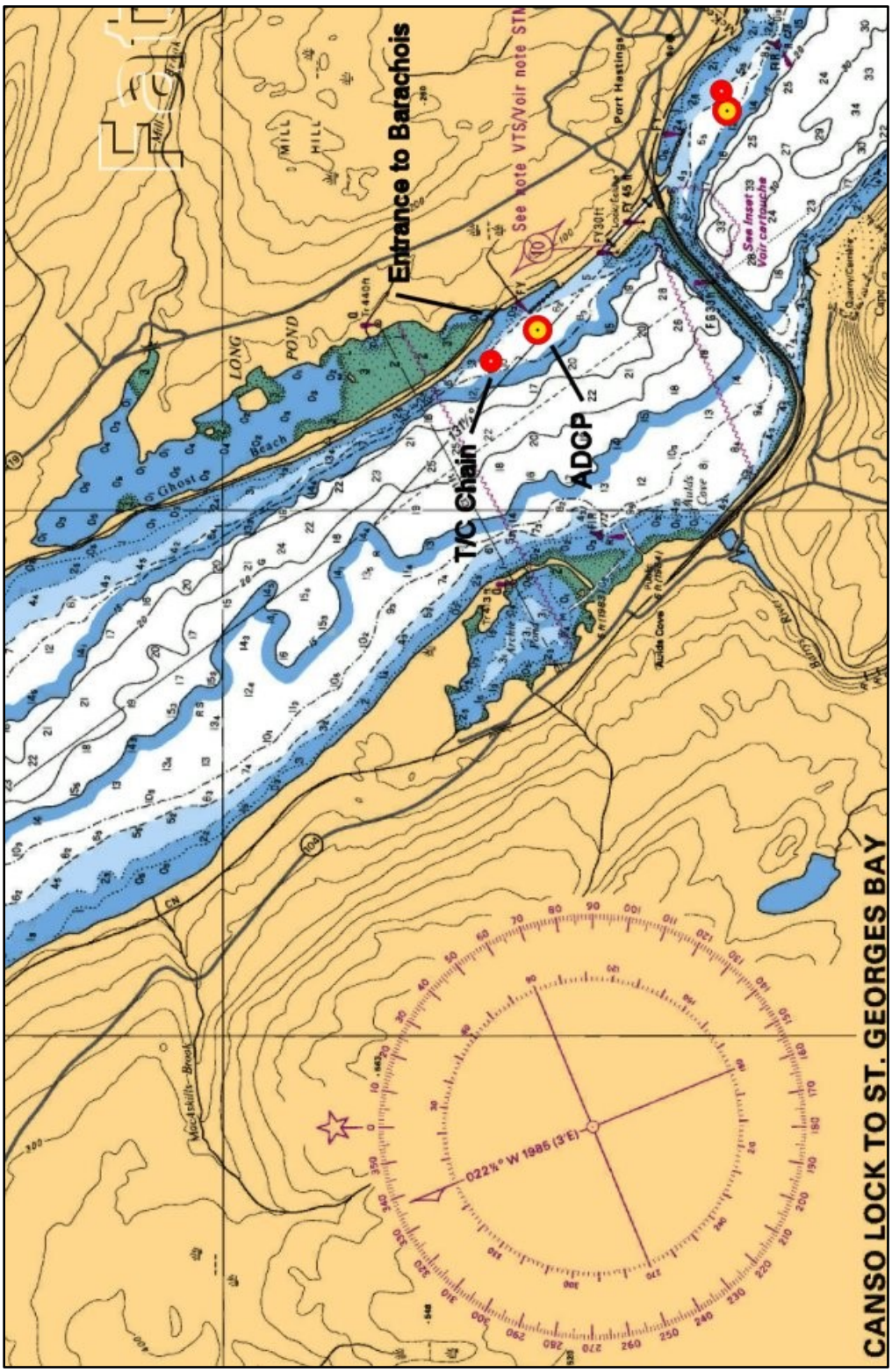

Figure 21: Location of Long Pond Barachois.

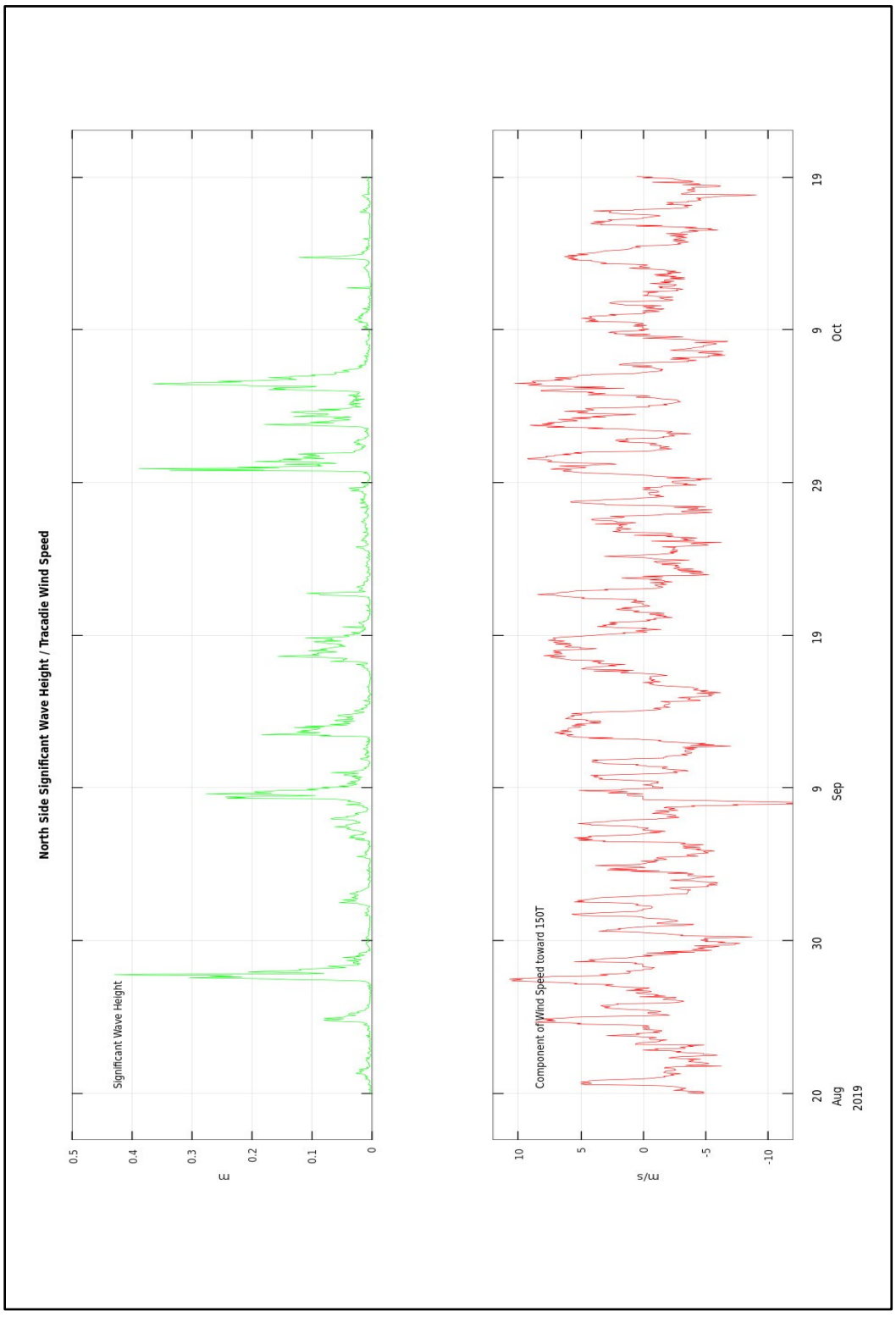

Figure 22: Tracadie Winds and Significant Wave Height North of the Causeway during the fall.

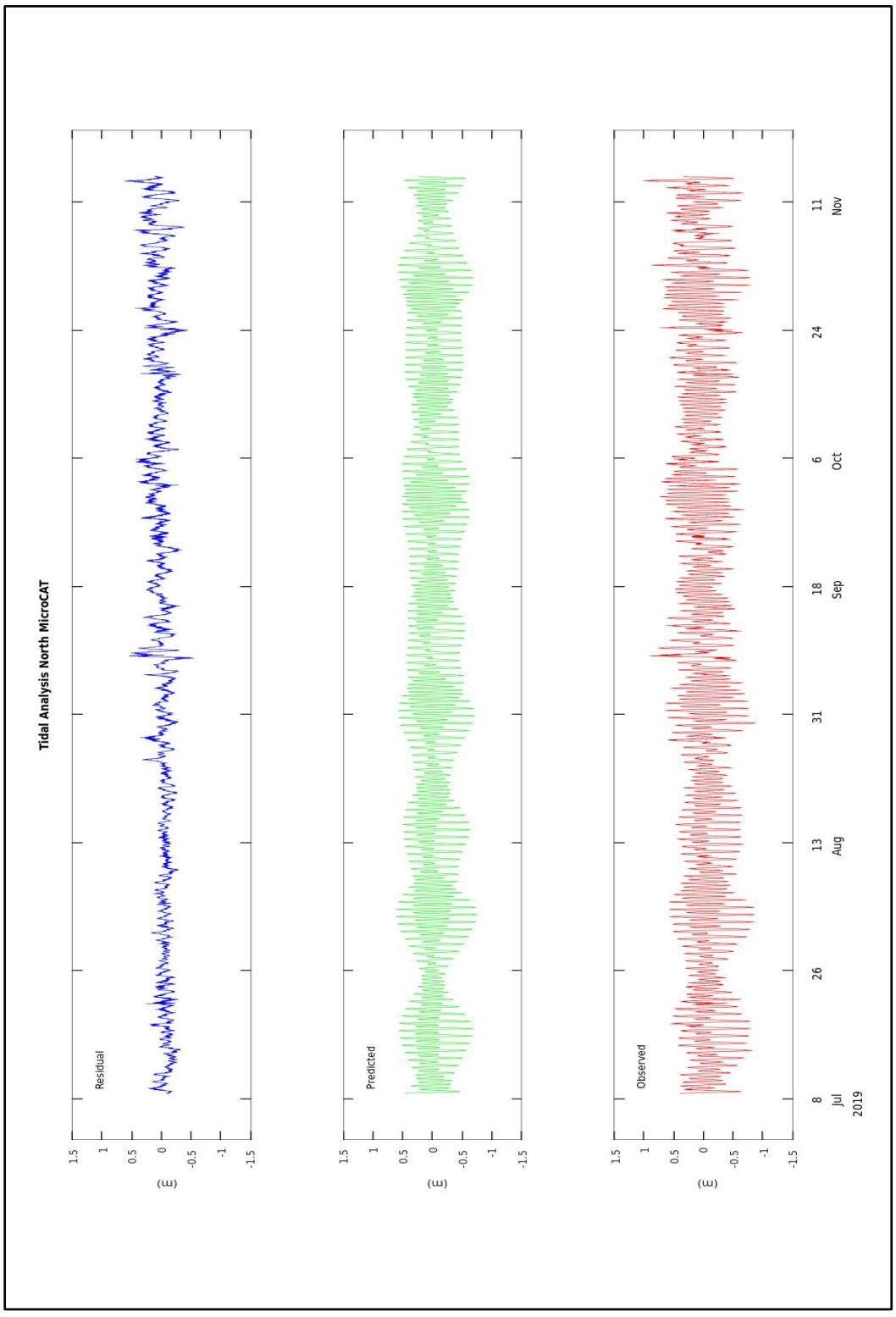

Figure 23: Results of Tidal Analysis of Northern MicroCAT Pressure Channel.

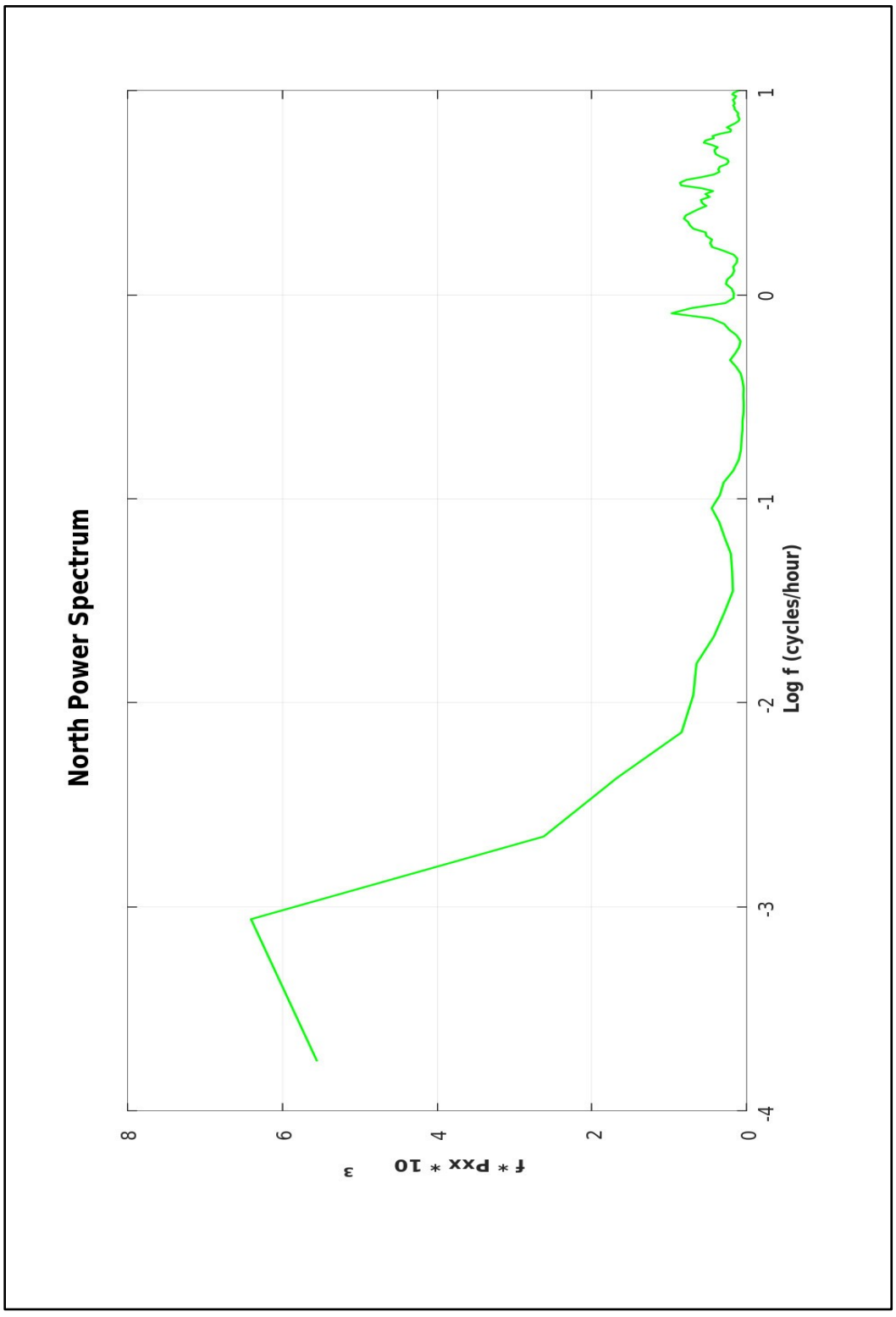

Figure 24: Power Spectra of Residual from Northern Tidal Analysis.

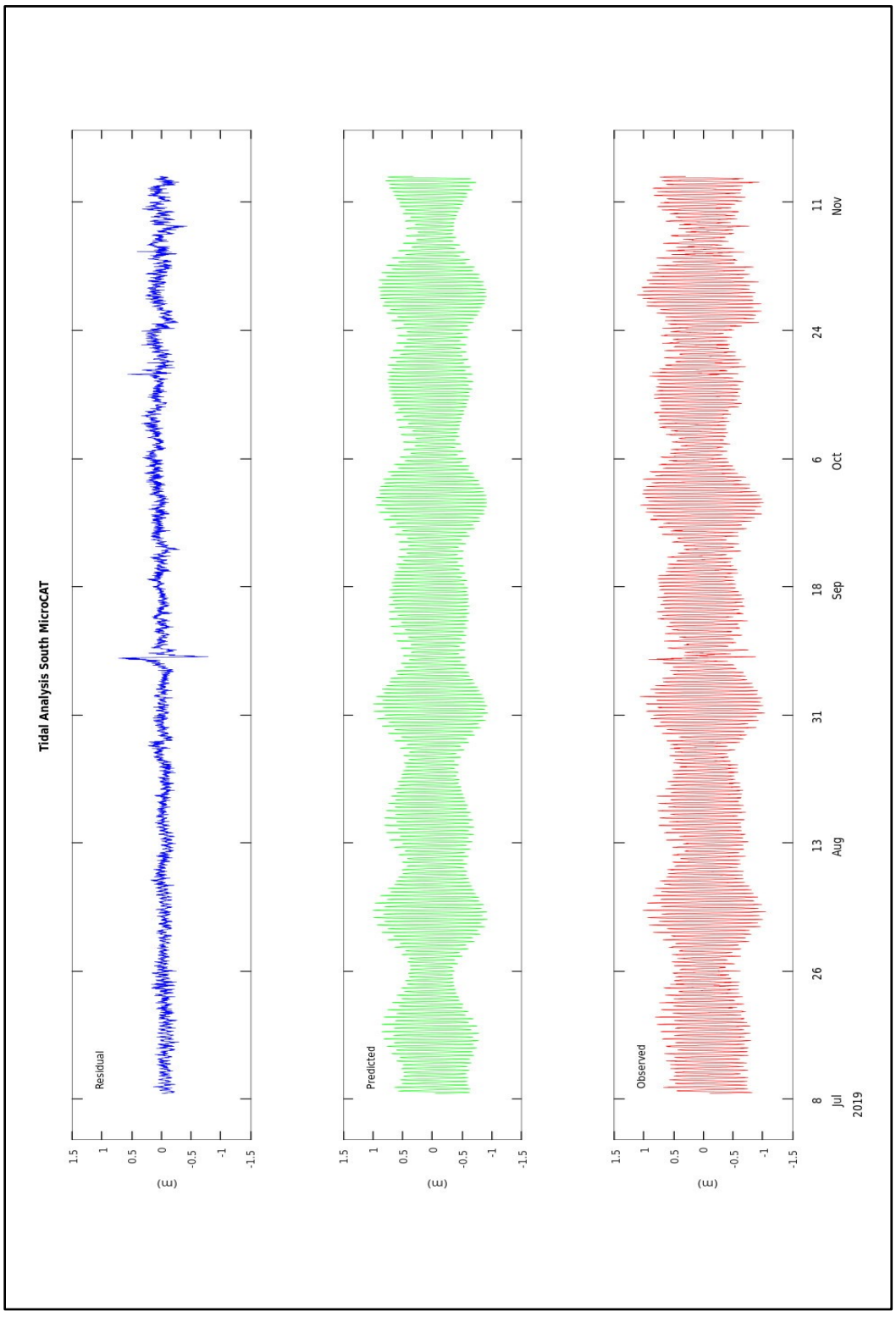

Figure 25: Results of Tidal Analysis of Southern MicroCAT Pressure Channel.

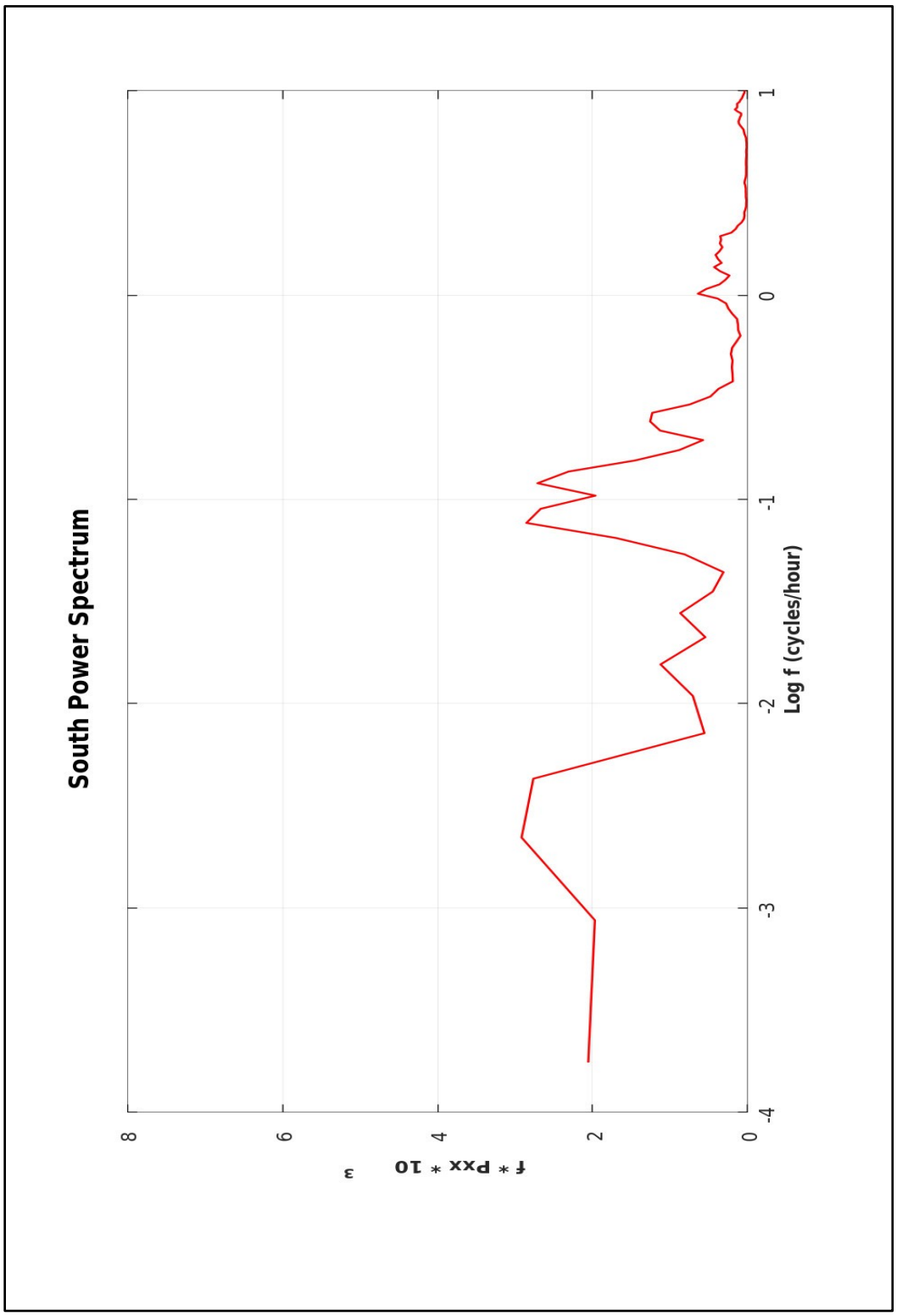

Figure 26: Power Spectra of Residual from Southern Tidal Analysis.

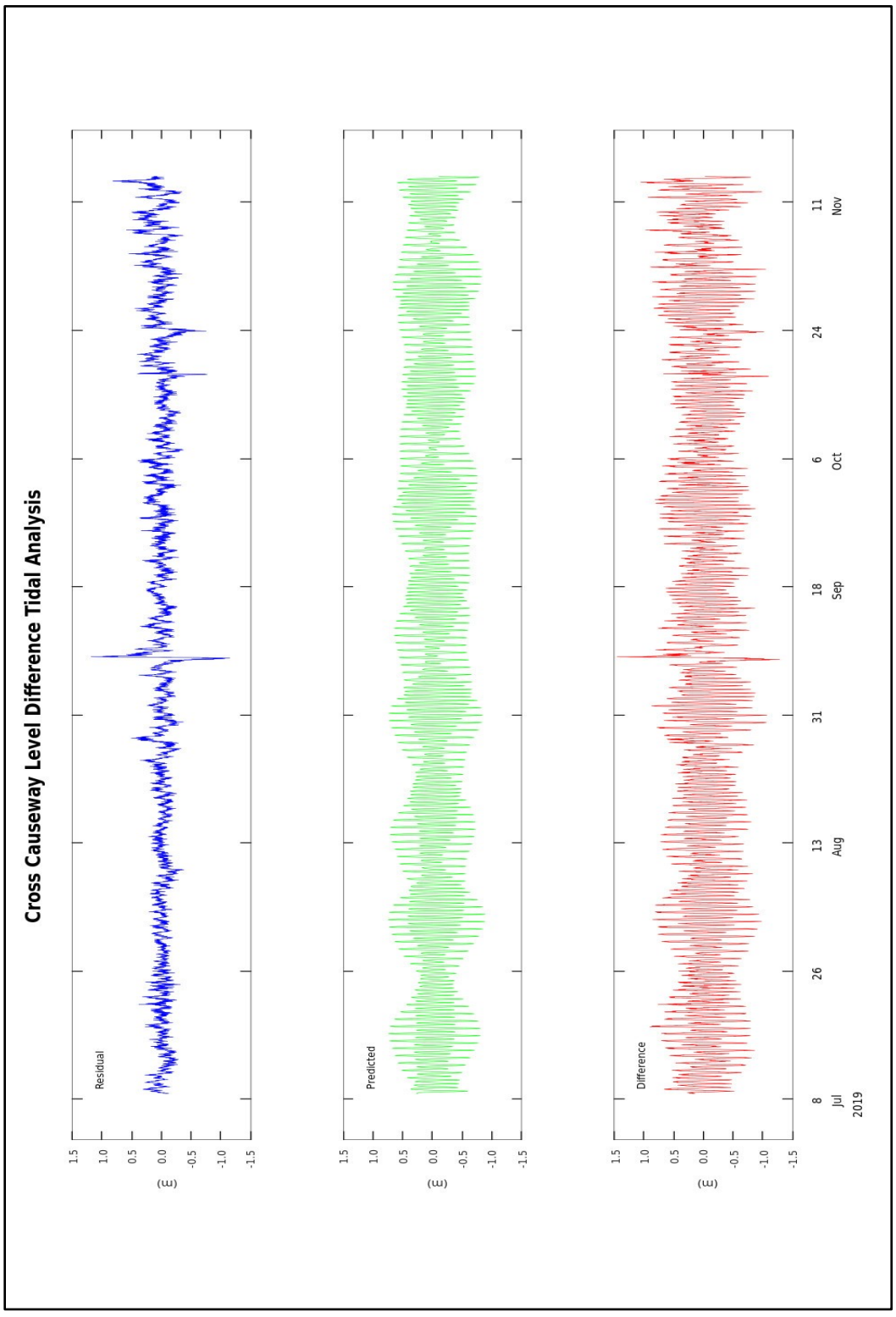

Figure 27: Results of Tidal Analysis of Cross-Causeway Water Level Difference

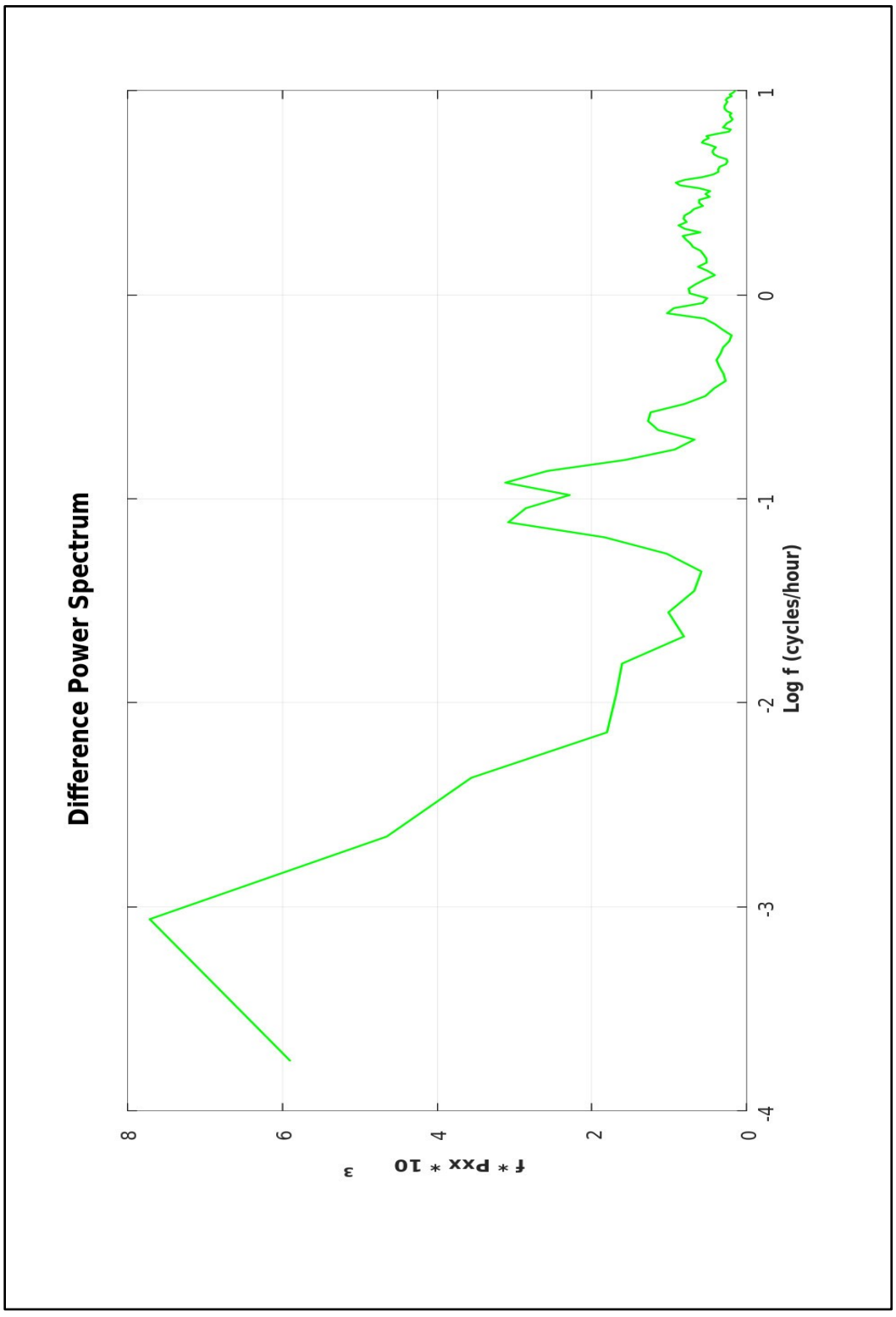

Figure 28: Power Spectra of Residual from Cross-Causeway Tidal Analysis.

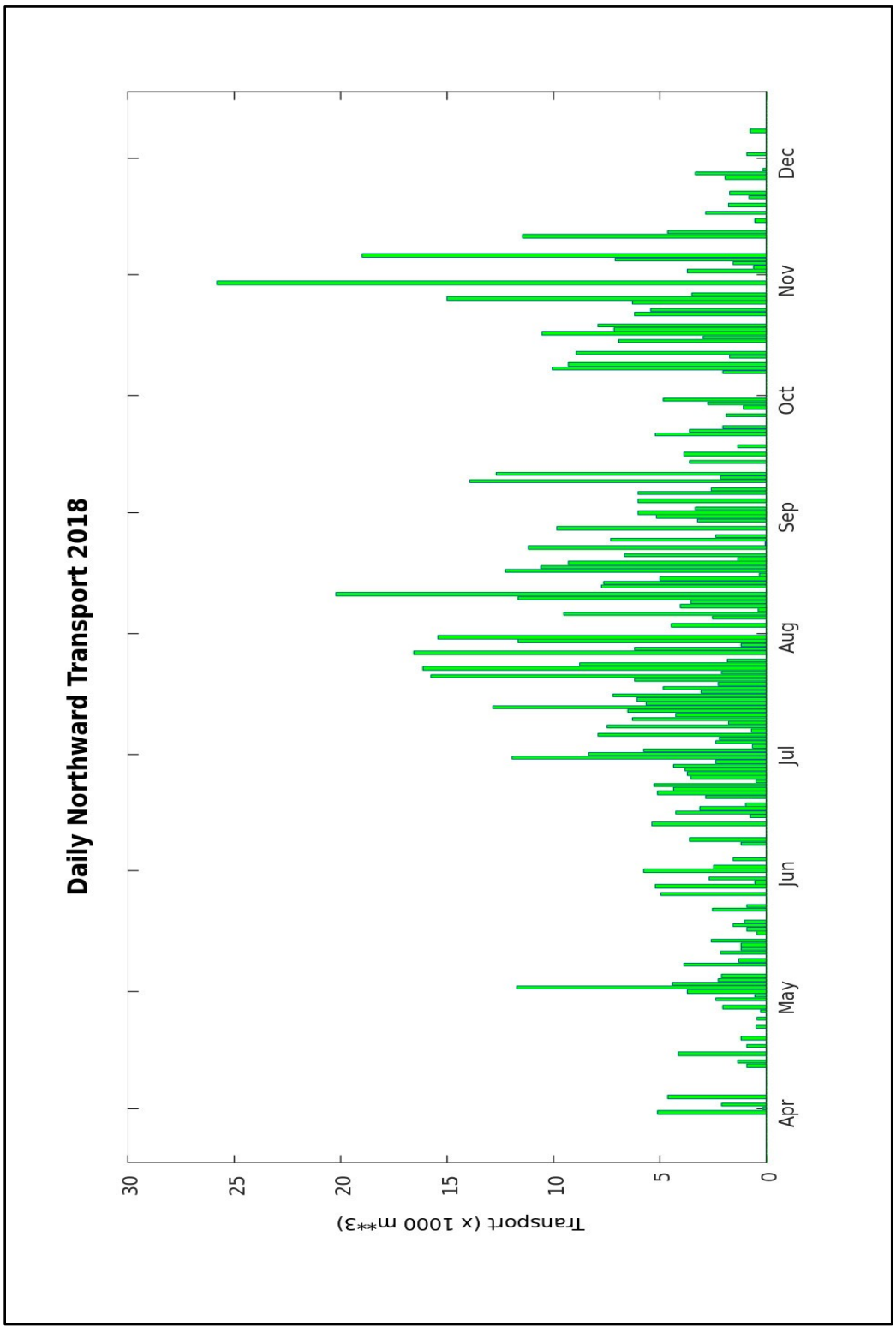

Figure 29: Daily Totals of Northward Transport Due to Lock Operation 2018.

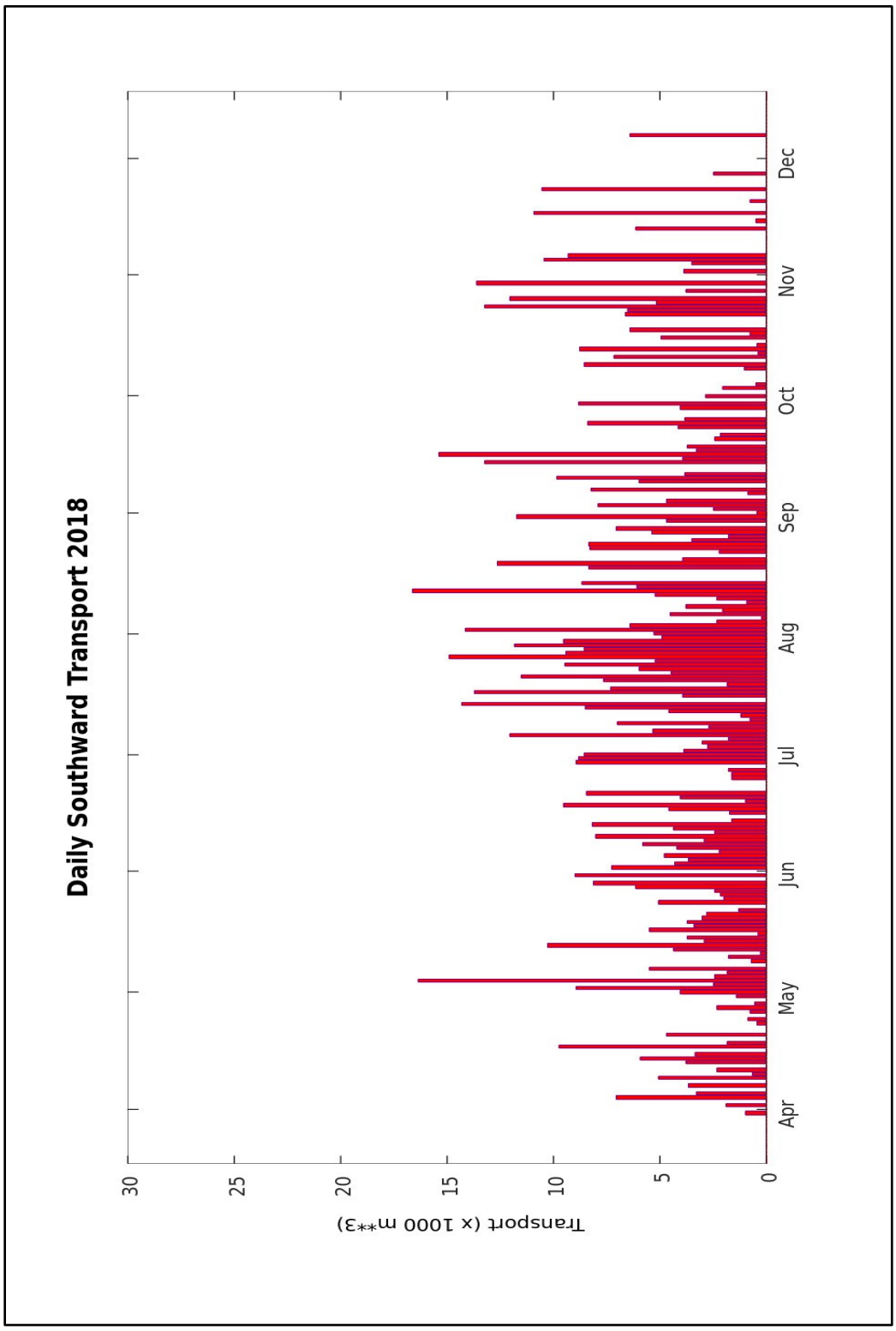

Figure 30: Daily Totals of Southward Transport Due to Lock Operation 2018.

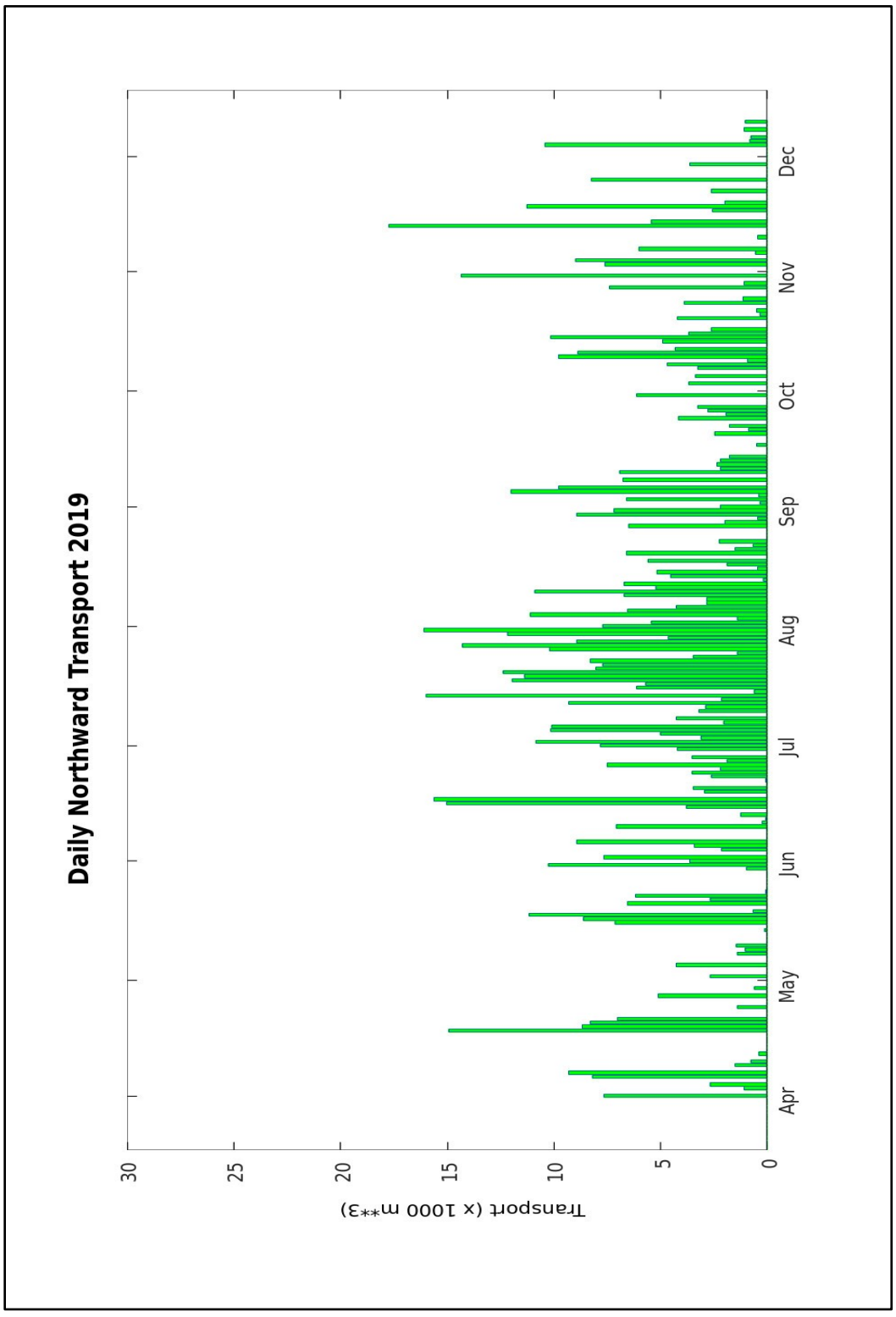

Figure 31: Daily Totals of Northward Transport Due to Lock Operation 2019.

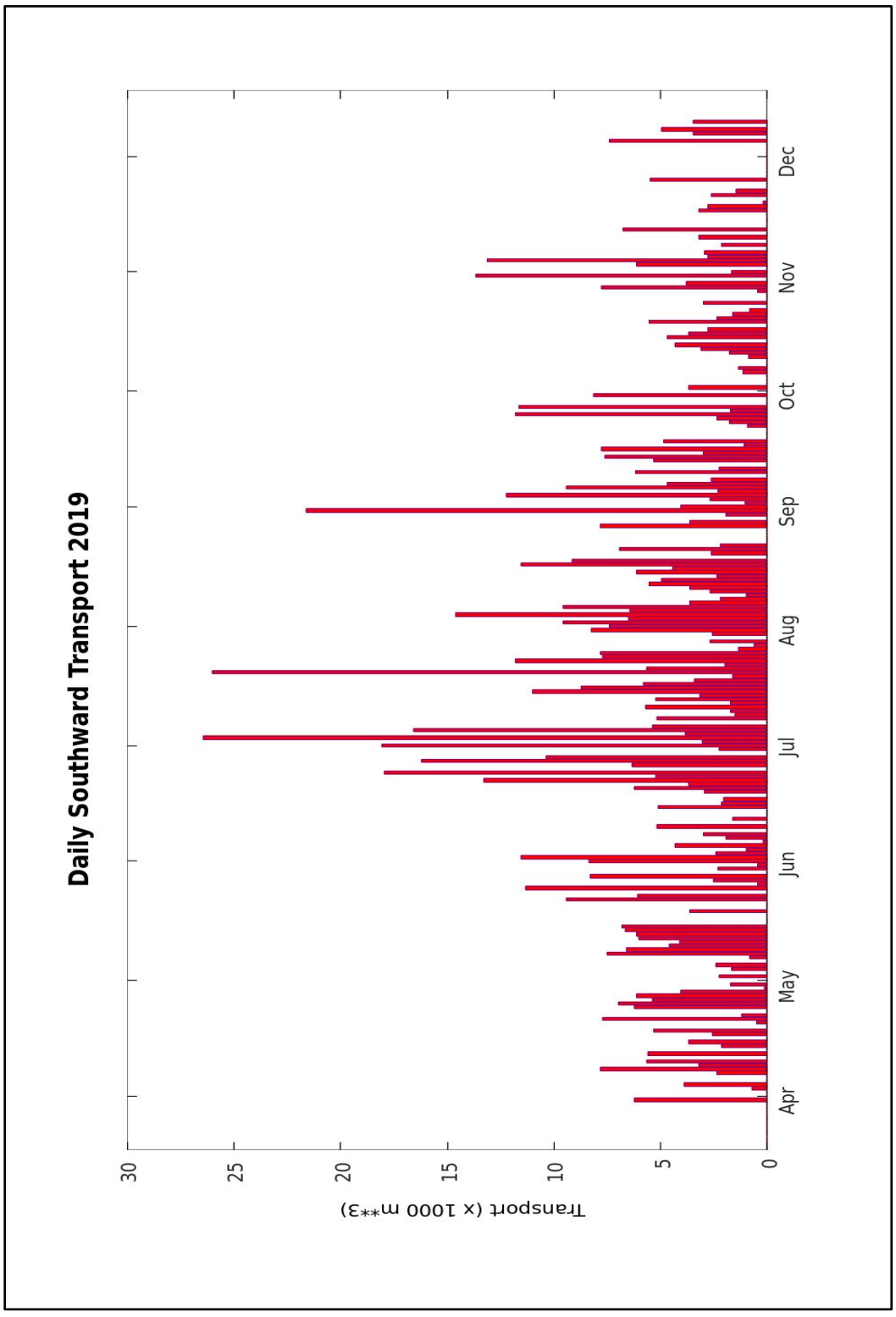

Figure 32: Daily Totals of Southward Transport Due to Lock Operation 2019.

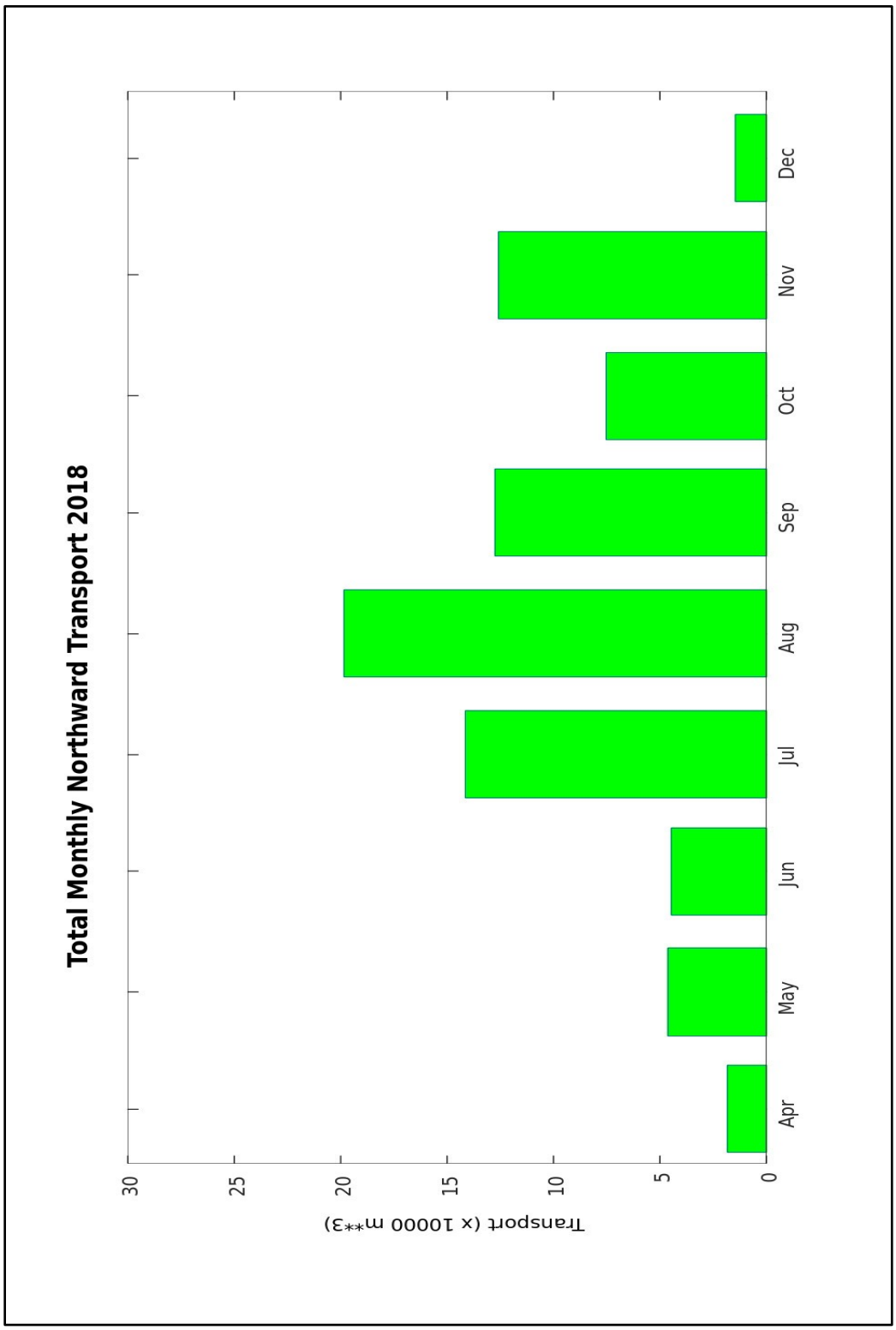

Figure 33: Monthly Totals of Northward Transport Due to Lock Operation 2018.

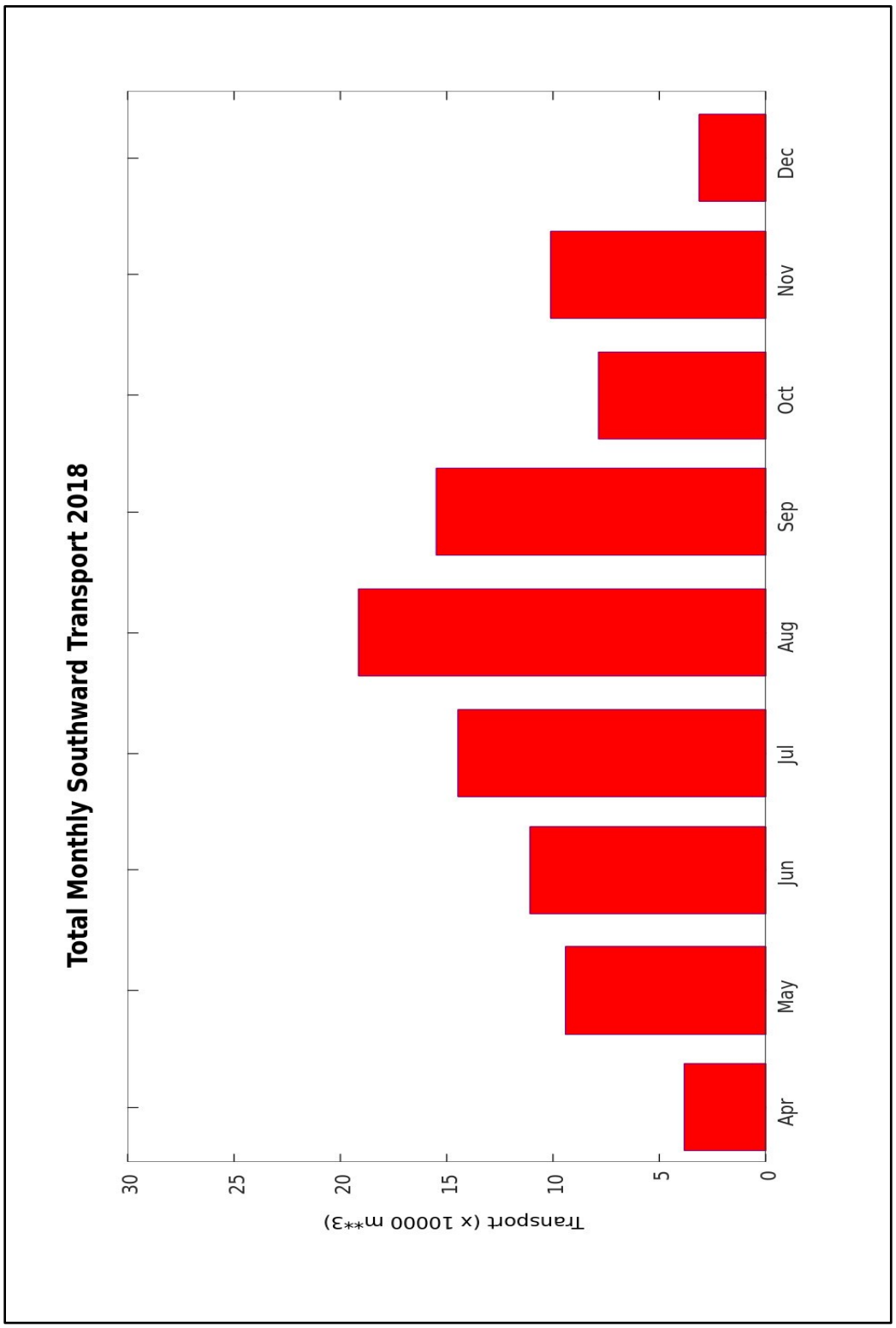

Figure 34: Monthly Totals of Southward Transport Due to Lock Operation 2018.

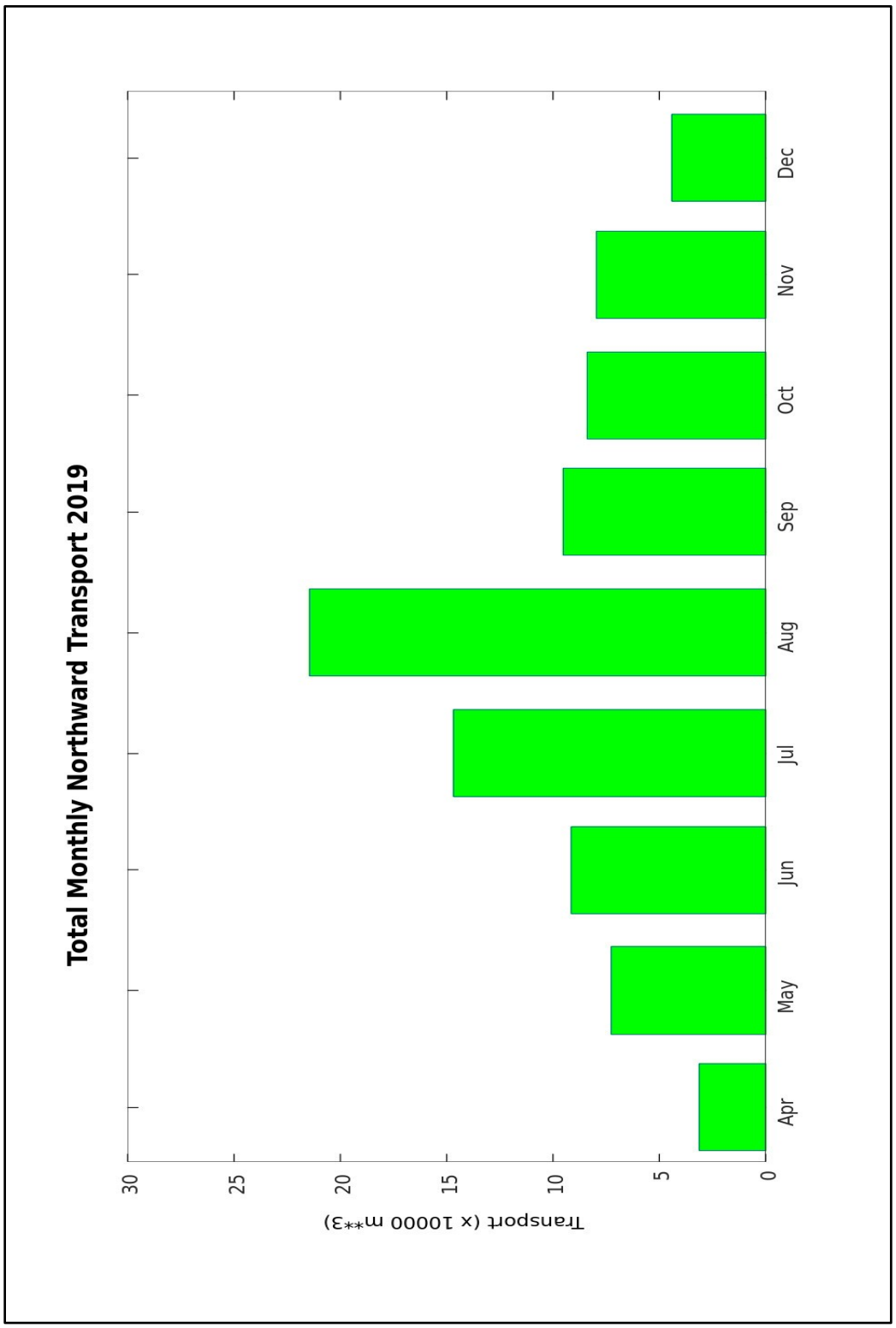

Figure 35: Monthly Totals of Northward Transport Due to Lock Operation 2019.

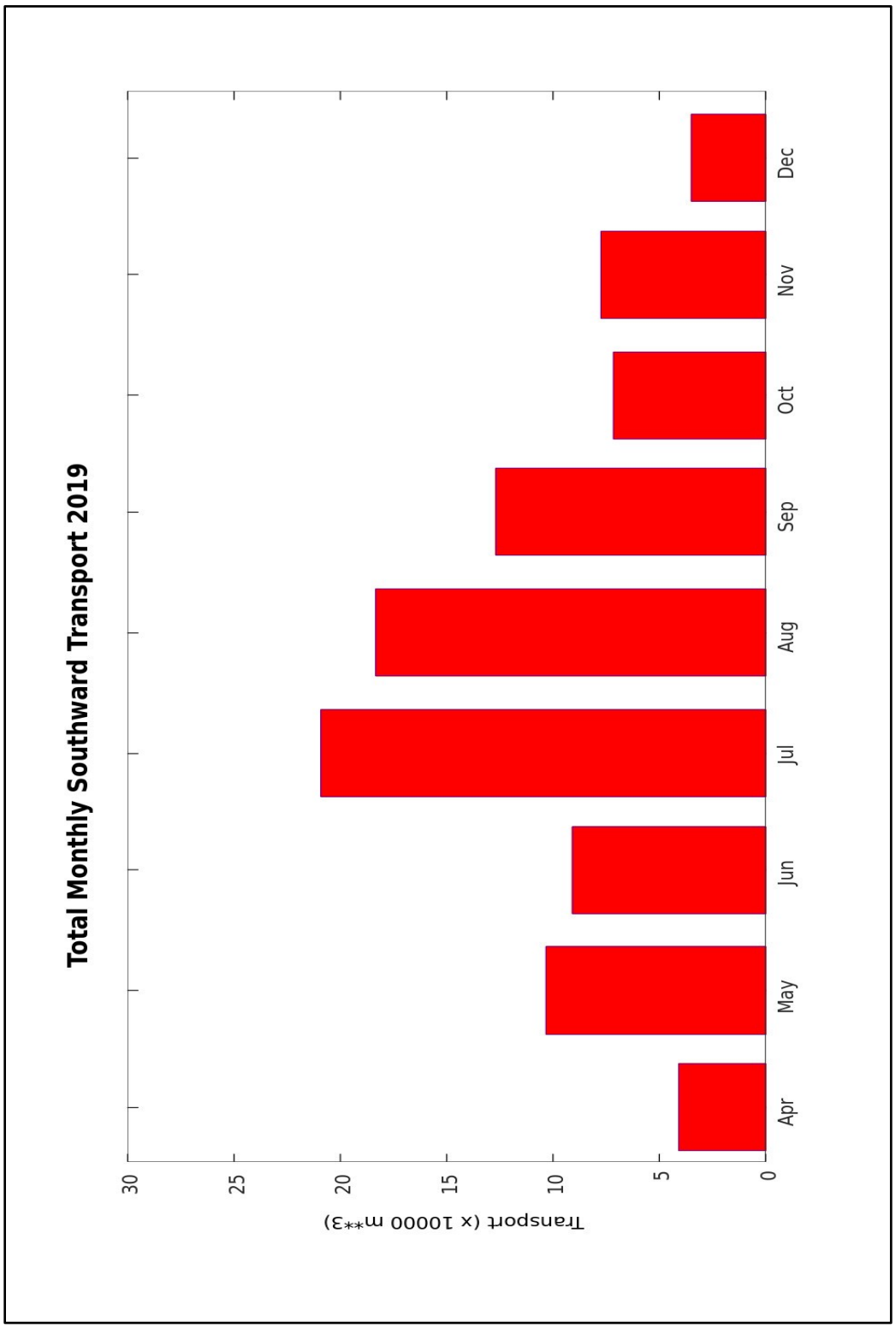

Figure 36: Monthly Totals of Southward Transport Due to Lock Operation 2019.

TABLES

Constituent	Amplitude (m)	Phase (UTC)
M2	0.29	26.2
O1	0.17	300.3
K1	0.15	339.0
S2	0.09	72.6
N2	0.07	356.3

Table 1: Five Largest Constituents from Tidal Analysis of Northern MicroCAT Pressure Channel.

Constituent	Amplitude (m)	Phase (UTC)
M2	0.59	345.9
S2	0.15	24.9
N2	0.14	323.2
K1	0.06	58.0
M4	0.05	252.8

Table 2: Five Largest Constituents from Tidal Analysis of Southern MicroCAT Pressure Channel.

Constituent	Amplitude (m)	Phase (UTC)
M2	0.41	138.5
K1	0.15	315.5
O1	0.14	287.7
S2	0.11	168.7
N2	0.09	116.5

Table 3: Five Largest Constituents from Tidal Analysis of Cross-Causeway Water Level Difference.

	Apr	May	Jun	Jul	Aug	Sep	Oct	Nov	Dec	Total
Northbound	23	40	62	102	107	49	36	34	19	474
Southbound	8	36	41	109	114	71	61	52	20	509

Table 4: Average Number of Locking Events 2016–2019.

Transit Direction	L=>H	L=>H	H=>L	H=>L
Initial Level	L	H	L	H
Final Level	H	H	L	L
Discharge	No	Yes	Yes	Yes

Table 5: Pattern of water discharged during locking events for various directions of transit and initial levels in the lock.